

SymBoltz.jl: a symbolic-numeric, approximation-free and differentiable linear Einstein-Boltzmann solver

Herman Sletmoen

Institute of Theoretical Astrophysics, University of Oslo, P.O.Box 1029 Blindern, N-0315 Oslo, Norway
e-mail: herman.sletmoen@astro.uio.no

Received XX / Accepted XX

ABSTRACT

SymBoltz is a new Julia package that solves the linear Einstein-Boltzmann equations. It features a symbolic-numeric interface for specifying equations, is free of approximation switching schemes and is compatible with automatic differentiation. Cosmological models are built from replaceable physical components in a way that scales well in model space, or alternatively written as one compact system of equations. The modeler should simply write down their equations, and SymBoltz solves them and eliminates friction in the modeling process. Symbolic knowledge enables powerful automation of tasks, such as separating computational stages like the background and perturbations, generating the analytical Jacobian matrix and its sparsity pattern, and interpolating arbitrary variables from the solution. Implicit solvers integrate the full stiff equations at all times without approximations, which greatly simplifies the code. Performance remains as good as in existing approximation-based codes due to high-order implicit methods that take long time steps, fast generated code, optimal handling of the Jacobian and efficient sparse matrix methods. Automatic differentiation gives exact derivatives of any output with respect to any input, which is important for gradient-based Markov chain Monte Carlo methods in large parameter spaces, training of emulators, Fisher forecasting and sensitivity analysis. The main features form a synergy that reinforces the design of the code. Results agree with established codes to 0.1% with standard precision. More work is needed to implement additional features and for fast reverse-mode automatic differentiation of scalar loss functions. SymBoltz is available at <https://github.com/hersle/SymBoltz.jl> with single-command installation and extensive documentation, and welcomes all contributions.

Key words. Cosmology: theory - Methods: numerical

Cosmology is at a crossroads (Freedman 2017). Despite the enormous success of the Λ CDM model in explaining many observations, the increasing precision of modern observations are revealing tensions between theory and observations. These suggest that the current standard model is not the ultimate truth.

On the theoretical side, this drives a search for the true cosmological model through modifications to Λ CDM (Bull et al. 2016). Efficiently exploring the space of models benefits from numerical tools that are easy to modify. Minimizing friction in the modeling process encourages relaxing model-dependent approximations, creating user-friendly interfaces and structuring codes with modular components that are easy to replace. Some of the most important such tools in the cosmological modeling toolbox are linear Einstein-Boltzmann solvers (“Boltzmann codes”) like CAMB (Lewis et al. 2000) and CLASS (Lesgourgues 2011a).

On the observational frontier, next-generation surveys like the Square Kilometer Array (Dewdney et al. 2009), Vera C. Rubin Observatory (LSST Science Collaboration 2009), Dark Energy Spectroscopic Instrument (DESI Collaboration 2016), Simon’s Observatory (The Simons Observatory Collaboration 2019) and Euclid (Euclid Collaboration 2025) promise more precise data. Setting models apart with upcoming data involves both theoretical model parameters and experimental nuisance parameters that coexist in large $O(100)$ -dimensional spaces (Piras et al. 2024). In high dimensions, modern Markov chain Monte Carlo methods like Hamiltonian Monte Carlo and the No-U-Turn Sampler (Hoffman & Gelman 2011) outperform the traditional Metropolis-Hastings algorithm (Hastings 1970). They explore parameter space more efficiently, but need both the likelihood

and its gradient with respect to parameters. Emulators have become popular to get this from existing non-differentiable codes by training differentiable neural networks to reproduce their output (e.g Bolliet et al. 2024; Bonici et al. 2024). Differentiability is also used in forward-modeling field-level inference with simulations and initial conditions from Boltzmann solvers, for example (Seljak et al. 2017). Automatic differentiation can compute derivatives more accurately and faster than approximate and brute-force finite differences. A differentiable Boltzmann solver is a cornerstone in the modern cosmological modeling toolbox.

SymBoltz is a new Boltzmann solver that aims to meet these needs, featuring a convenient symbolic-numeric interface, approximation-freeness and differentiability. At its core, a Boltzmann code solves the Einstein equations for a gravitational theory coupled to some particle species described by Boltzmann equations up to first perturbative order around a homogeneous and isotropic universe. For example, it predicts cosmic microwave background (CMB), baryon acoustic oscillation (BAO) or supernova (SN) observations, or generates initial conditions for non-linear N -body simulations of large-scale structure.

This article is structured as follows. Section 1 motivates SymBoltz by reviewing the historical development of Boltzmann codes and methods for computing derivatives. Section 2 describes the structure and main features of SymBoltz and how it differs from other codes. Section 3 shows example usage. Section 4 compares performance to an existing code. Section 5 describes possibilities for future work. Section 6 concludes with the current state of the code. Appendices A to C list equations, implementation details, comparison settings and testing methods.

1. History and motivation

Peebles & Yu (1970) were first to numerically integrate a comprehensive set of linear Einstein-Boltzmann equations. Their work was refined over several years, and Ma & Bertschinger (1995) established the groundwork for modern Boltzmann solvers with their code COSMICS. Seljak & Zaldarriaga (1996) soon realized that one can integrate photon multipoles by parts to reduce many differential equations to one integral solution and released CMBFAST. Their line-of-sight integration method has become a standard technique that greatly speeds up the calculation, but requires truncating the multipoles in the differential equations. This Fortran codebase has since evolved into CAMB¹ written by Lewis et al. (2000), which is one of the two most used and maintained Boltzmann solvers today. Doran (2005a) ported CMBFAST to C++ with the fork CMBEASY, which structured the code in an object-oriented fashion and improved user-friendliness, but this project is abandoned today.

Lesgourges (2011a); Blas et al. (2011) started the second major family of Boltzmann solvers with the birth of CLASS² in C. It improved performance, user-friendliness, code flexibility, ease of modification and control over precision parameters. It was the first cross-check of CAMB from an independent branch and boosted the scientific accuracy of the Planck mission.

Since then a healthy arms race have fueled refinements to CAMB and CLASS. Both codes have spawned many forks for studying alternative models and performing custom calculations. Today they are very well-made, efficient and reliable tools.

Recently, several alternative solvers have appeared on the market. They target new numerical techniques, lack of approximations, differentiability, GPU parallelization, interactivity and symbolic computation. PyCosmo³ by Refregier et al. (2018) in Python was the first symbolic-numeric Boltzmann code that generates fast C++ code from user-provided symbolic equations, optimizes the sparse and analytical Jacobian matrix and avoids approximation schemes. Bolt.jl⁴ by Li et al. (2023) in Julia is also approximation-free, supports forward-mode automatic differentiation and uses similar differential equations solvers as SymBoltz. DISCO-EB⁵ by Hahn et al. (2024) in the JAX framework in Python is also differentiable and relaxes approximation schemes to avoid overhead from switching equations on GPUs. SymBoltz.jl⁶ is inspired by all these developments.

1.1. Structure of traditional Boltzmann solvers

The full Einstein-Boltzmann equations are partial differential equations that linearize to ordinary differential equations.

In principle, the core task of a Boltzmann solver is thus very simple: to solve these ordinary differential equations (ODEs) $d\mathbf{u}/d\tau = \mathbf{f}(\tau, \mathbf{u}, \mathbf{p})$ for some initial conditions $\mathbf{u}(\tau_0)$ and parameters \mathbf{p} , including several perturbation wavenumbers, and compute desired quantities from their solution, like power spectra.

In practice, however, several properties complicate this task. First, the equations separate into computational stages that benefit substantially from being solved sequentially for performance and stability, such as the background and perturbations stages. It is common to solve each stage with interpolated input from the previous stage, and joining these can be cumbersome and frag-

ment code. Second, the set of equations is very long and convoluted. Ideally, parts of the equations should be easily replaceable to accommodate different submodels for gravity and particle species. Organizing a code with a suitable modular structure that scales well in model space is hard. Third, wildly different timescales coexist in the equations and make them extremely stiff and intractable to solve with standard explicit ODE solvers. This stiffness must be massaged away in the equations or dealt with numerically in other ways. Fourth, the size of differential equations is very large and increases for more accurate description of relativistic species. Typical models with accurate treatment of photons and neutrinos need $O(100)$ equations. Fifth, the perturbations must be solved for many different wavenumbers k , and tradeoffs between performance and precision must be made.

To overcome these challenges, most Boltzmann solvers are written in low-level high-performance languages like C, C++ and Fortran. They are tightly adapted to the pipeline-like computational structure of the problem (e.g. input → background → thermodynamics → perturbations → ... → output in Lesgourges (2011a)). This makes sense for programmers, but does not necessarily provide the simplest interface for modelers.

Traditional codes like CAMB and CLASS have nonexistent or thin abstraction layers. To modify them, users must work directly in the low-level numerical code and have a good understanding of its internal structure. For example, to implement a new species, one must often modify the code in many places: input handling for new parameters, new background equations, new thermodynamics equations, new perturbation equations, joining each of these stages, output handling, and so on. This leads to fragmented code where changes related to one species are scattered throughout the code.

This structure scales poorly in model space. As more species or gravitational theories are added, each module becomes intertwined with code from other physical components. Even if deactivated by if statements at runtime, their mere presence in the source code increases its complexity and reduces its readability.

One can alleviate this problem to some extent by instead forking the code for modified models, so the main code base is not polluted. But this just moves the problem. Forking duplicates the entire code base even though only small parts are modified. Forks are often abandoned and do not receive upstream improvements. They are also incompatible with each other unless one merges them into one code, but then one is back to the first problem.

The two-language problem amplifies the problem, as data analysis often happens in slow high-level languages like Python. This shapes Boltzmann solvers to rigid pipelines that must compute everything at once and avoid intercession at all costs, in order to maximize performance in the low-level language before passing output back to the high-level language. Some features are really just post-processing of the ODE solutions, but are appended to the pipeline even if peripheral to the core task of an Einstein-Boltzmann solver – solving the Einstein-Boltzmann equations. Features like non-linear boosting and CMB lensing could be made as smaller and interoperating modular packages, but instead become part of “all-in-one” Boltzmann codes.

These patterns lead to big monolithic Boltzmann solvers. They become increasingly complex as they incorporate more models and features beyond their original core scope. This complexity has even driven development of specialized AI assistants for CLASS (Casas et al. 2025). While existing Boltzmann solvers are impressively well-engineered and such tools are only helpful, we think these are symptoms of unnecessary complexity.

¹ <https://camb.info/>

² <http://class-code.net>

³ <https://pypi.org/project/PyCosmo/>

⁴ <https://github.com/xzackli/Bolt.jl>

⁵ <https://github.com/ohahn/DISCO-EB>

⁶ <https://github.com/hersle/SymBoltz.jl>

1.2. Boltzmann solver approximation schemes

The Einstein-Boltzmann equations are infamously stiff (Nadkarni-Ghosh & Refregier 2017). This property of differential equations means their numerical solution is unstable with standard explicit integrators and requires tiny step sizes, making them hard to solve. Stiffness can arise when multiple and very different time scales appear in the same problem. This is very common in cosmology, where particles interact very rapidly in a universe that expands very slowly, particularly in the tightly coupled baryon-photon fluid, for example. Stiff equations are practically impossible to integrate with explicit solvers and require special treatment.

For a long time, Boltzmann solvers have massaged away stiffness with several approximation schemes⁷ in the equations (e.g. Doran (2005b); Blas et al. (2011); Lewis (2025)):

- tight-coupling approximation (TCA),
- ultra-relativistic fluid approximation (UFA),
- radiation streaming approximation (RSA),
- non-cold dark matter fluid approximation (NCDMFA),
- Saha approximation.

They involve switching from one set of equations to another when some control variable measuring the applicability of the approximation crosses a threshold. This can change the variables in the ODE and require reinitializing it. Approximations can help both speed and stability and allow the use of explicit solvers.

However, approximations put much more strain on modelers to derive and validate several versions of the equations in different regimes. This process may have to be repeated when the model is modified. The numerics also become more complicated: timeseries from each ODE solution must be stitched together, each separate ODE system can use different tolerances, ODE integrators must be reinitialized, and so on.

Another way to integrate stiff equations is to use appropriate implicit solvers. PyCosmo first solved the full stiff Einstein-Boltzmann equations with an implicit integrator, followed by Bolt.jl and DISCO-EB. CLASS also has an implicit solver, but does not permit disabling the tight-coupling approximation, for example. Historically, implicit solvers may have been underutilized because they are harder to implement than explicit solvers and have a reputation for being slower, and due to iterative evolution from initial Boltzmann codes that were centered around approximations. However, new life has recently been breathed into the field of implicit solvers, with development of new methods combined with techniques like automatic and symbolic differentiation that make them more feasible and powerful (e.g. Steinebach 2023; Ekanathan et al. 2025).

1.3. Differentiation methods

Derivatives are important in computing. Cosmological applications are no exception. For example, algorithms that optimize likelihoods and Markov chain Monte Carlo (MCMC) samplers for Bayesian parameter inference can take advantage of derivatives of the likelihood with respect to each parameter to intelligently step in a direction where the likelihood increases. In machine learning, the same applies when training neural networks emulators for cosmological observables as functions of parameters by minimizing a scalar loss. Some cosmologies

are parametrized as boundary-value problems with the shooting method, and use nonlinear root solvers like Newton’s method that need Jacobians. Implicit ODE solvers also use Jacobians to solve for values at the next time step. Fisher forecasting uses the Hessian (double derivative) of the likelihood with respect to parameters to predict how strong parameter constraints that can be placed by data with some uncertainty. Boltzmann solvers save time by interpolating spectra computed on coarse grids of k and l to finer grids, and this can be made more precise with derivatives with respect to k and l . These are all examples where (applications of) Boltzmann solvers need derivatives.

There are at least four ways to compute derivatives.

Manual differentiation is human application of differentiation rules, but is limited to simple expressions and by human error.

Symbolic differentiation automates this process with computer algebra systems, but is inherently symbolic and cannot differentiate arbitrary programs nested with control flow like conditional statements and loops that depend on numerical values.

Finite differentiation approximates the derivative $f'(x) \approx (f(x + \epsilon/2) - f(x - \epsilon/2)) / \epsilon$ with a small $\epsilon > 0$ (here using central differences) by simply evaluating the program several times. This can differentiate arbitrary programs, but is approximate, introduces the step size ϵ as a hyperparameter that must be tuned for both accuracy and stability, and is a brute-force approach that requires $O(n)$ evaluations ($2n$ using central differences) to compute the gradient of an n -variate scalar f .

Automatic differentiation can be understood by viewing any computer program as a (big) composite function

$$f = f_N \circ f_{N-1} \circ \cdots \circ f_2 \circ f_1 = f_N(f_{N-1}(\cdots f_2(f_1))) \quad (1)$$

of (many) elementary operations $f_i : \mathbb{R}^{a_i} \rightarrow \mathbb{R}^{b_i}$ (think of f_i as the i -th line of code). It then numerically evaluates the chain rule

$$J = J_N \cdot J_{N-1} \cdots J_2 \cdot J_1. \quad (2)$$

through the Jacobian $(J_n)_{ij} = \partial f_{n,i} / \partial f_{n-1,j}$ of every elementary operation to accumulate the derivative of the entire program. This is numerically exact, free of precision parameters, usually requires fewer operations than finite differences, but is perhaps less intuitive, harder to implement and needs the source code of the program (1) to interpret it in the non-standard way (2).

Notably, while the function (1) must be evaluated inside-to-outside (right-to-left), the chain rule (2) is an associative matrix product that can be evaluated in any order. This generally changes the number of operations and is a more open-ended computational problem. Forward-mode automatic differentiation seeds $J_1 = \mathbf{1}$ (the derivative of the input with respect to itself) and multiplies $J_N(J_{N-1}(\cdots (J_2(J_1))))$ by “pushing” every column of J_1 forward through the product in the same evaluation order as f . Reverse-mode first computes f in a forward pass, then seeds $J_N = \mathbf{1}$ (the derivative of the output with respect to itself) and multiplies $((J_N)J_{N-1} \cdots J_2)J_1$ by “pulling” every row of J_N backwards through the product. This usually makes forward-mode faster when $f : \mathbb{R}^a \rightarrow \mathbb{R}^b$ has more outputs $b \gg a$, and reverse-mode better when there are more inputs $a \gg b$.

In practice, both modes are implemented using techniques like operator overloading or source code transformation. The former specializes every function on a particular “dual number” that computes both the value and derivative of the function (e.g. Revels et al. 2016). The latter analyzes the source code for f and transforms it into another code that computes J . In any case, automatic differentiation requires access to the source code!

⁷ Here “approximations” refers to schemes that switch between different equations at different times. It excludes techniques like multipole truncation and line-of-sight integration, which SymBoltz also uses.

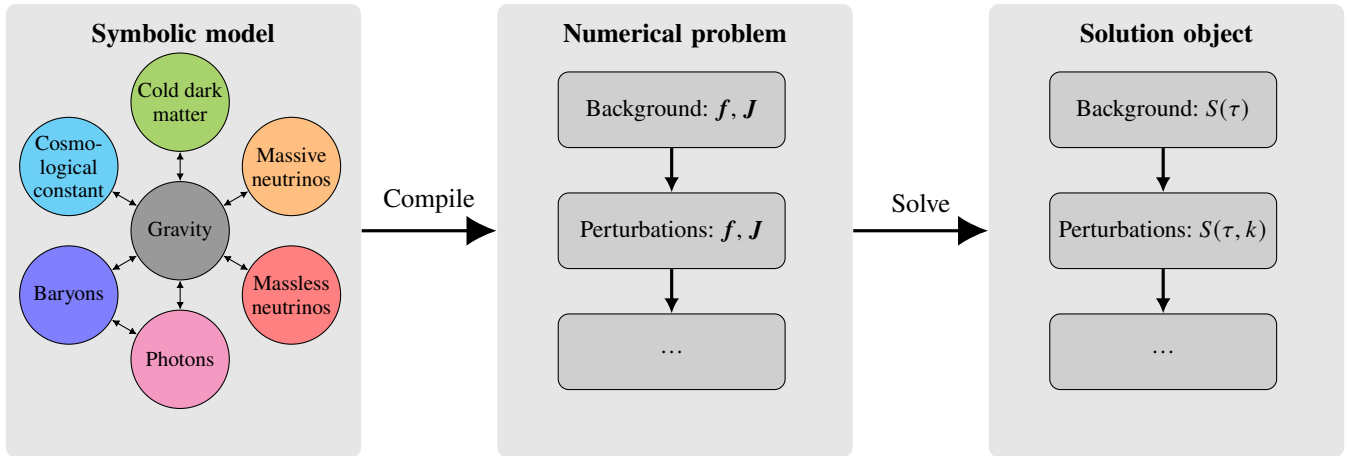


Fig. 1. SymBoltz represents cosmological models with symbolic equations grouped in physical components for the metric, gravity and particle species. This is compiled to a numerical problem that splits equations into background and perturbation stages and generates fast code for ODE functions f and Jacobians J . The problem is then solved and the result stored in a solution object that gives access to any variable S in the model.

2. Code architecture and main features

SymBoltz is designed around three main features. In short, it has a symbolic-numeric abstraction interface where users enter high-level symbolic equations, and automatically compiles them to fast low-level numerical functions. It cures stiffness with implicit ODE solvers, and uses no approximation schemes to keep models simple, elegant and extensible. It is differentiable, so one can get accurate derivatives of any output with respect to any input. This provides rapid model prototyping, helpful abstractions and automates tasks one must do manually when modifying other codes. SymBoltz encourages interactive use and pursues a modular design that lets users integrate what they need from the package into their own applications. The end goal is to prioritize the modeler, who should be able to just write down their equations while SymBoltz handles modeling chores.

The code is written in the Julia programming language (Bezanson et al. 2017), with a rich ecosystem of scientific packages and an aim to resolve the two-language problem. The symbolic-numeric interface is built on ModelingToolkit.jl (Ma et al. 2022) and Symbolics.jl (Gowda et al. 2022). The compiled functions are integrated by implicit ODE solvers in OrdinaryDiffEq.jl (Rackauckas & Nie 2017). Automatic differentiation works through ForwardDiff.jl (Revels et al. 2016).

The next subsections describe SymBoltz' three main features in more detail. Other implementation details are given in appendix A. **This paper is as of SymBoltz version 0.14.1. Please see the package documentation for definitive up-to-date information.**

2.1. Symbolic-numeric interface

The core of SymBoltz is built around a symbolic-numeric interface illustrated in fig. 1. Variables and equations are specified in a high-level user-friendly symbolic modeling language, then compiled down to low-level numerical code that is integrated by ODE solvers. With knowledge of the symbolic equations, SymBoltz can analyze their structure programmatically to ease model specification, automate related boilerplate tasks and generate fast and stable code that avoids approximations.

We think three properties motivate some kind of symbolic abstraction layer around the Einstein-Boltzmann equations.

First, the equations are most easily written as one large ODE, but optimally solved as several ODEs in stages like the background, perturbations and line-of-sight integration. Mathematically, the Jacobian matrix of this single ODE encodes which variables are independent and belong to which stages. It is easiest for modelers to specify equations in one common system, where the perturbations can refer to variables in the background, for example. The separation into computational stages can be automated.

Second, solving each stage is hard due to stiffness, performance requirements and its dependence on previous stages. To overcome this, it is helpful to automatically generate ODE code that is optimal in speed, accuracy and stability, generate the ODE Jacobian needed by implicit solvers and interpolate variables from previous stages. Modelers should not worry about this.

Third, the equations are often modified because the true cosmology is unknown. This can be made easier by organizing equations in a way that reflects the physical structure of the model, so it is easy to replace a related subset of equations with another without duplicating the entire model. This could be slow to do at the numerical level, but can be done with no runtime penalty in an intermediate symbolic representation of the equations.

Inspired by this, SymBoltz inverts the traditional layout of Boltzmann solvers. While most codes are built as pipelines that follow the background, perturbations and other stages of the equations, SymBoltz is primarily structured around the physical components that they consists of. Related variables and equations are grouped in distinct components for the metric, gravitational theory, photons, baryons, dark matter, dark energy, neutrinos and other species (see fig. 1). This isolates everything related to one submodel to one place. Any set of such submodels are joined into a full cosmological model, like Λ CDM. Interactions (e.g. Compton scattering or sourcing of gravity) are equations between components. Adding new submodels is easy, and SymBoltz is largely devoted to simply building a well-organized library of them.

SymBoltz then takes a full cosmological model, separates it into stages and generates numerical code to solve each stage. This preprocessing does not slow the code at runtime; to the contrary the symbolic equations give extra information like the Jacobian that enhances speed and stability. Modifications automatically enjoy these benefits without extra user input.

The modular component-based structure scales well in model space. For example, modified gravity or dark energy models can be written down as self-contained submodels and combined with

other components to create many different extended cosmological models. The generic symbolic framework can also be used to build reduced models with non-interacting radiation, matter and dark energy species. When exploring modified gravity theories, it can be helpful to test such toy models to understand how gravity responds to pure fluids without coupling to baryons and photons.

In contrast, the monolithic layout of traditional codes scatter changes related to one submodel across different modules for input/output, the background, perturbations and so on. As more and more submodels are added, the code is increasingly intertwined and fragmented. They are also not flexible enough to test simpler toy models, as baryons and photons are hardcoded as fundamental to the structure of the code. This design fits the computational structure better than the physical one. It can result in an overwhelming code that becomes hard to read and modify, and whose complexity scales poorly in model space.

As an alternative to component-based modeling, SymBoltz also includes a version of the default Λ CDM model with all equations packed into one big “unstructured” system. This makes it trivial to change anything in the equations, but sacrifices modularity. The symbolic interface makes it very compact: SymBoltz defines a full Λ CDM model in just 277 straightforward lines of code⁸, while the equivalent code to browse in CLASS is spread over 10 files with 27721 lines⁹.

PyCosmo’s symbolic interface also generates code for ODEs and sparse Jacobians, but does not focus on component-based modeling or automating tasks like stage separation, for example.

SymBoltz’ symbolic-numeric interface simplifies solving and modifying the Einstein-Boltzmann equations. It aims to maximize speed, stability and convenience with minimal user input. The next sections go into detail on how this is done. Section 3.2 shows a concrete example and some of its features in action.

2.1.1. Automatic numerical code generation

SymBoltz automatically compiles symbolic equations to numerical code for ordinary differential equations (ODEs)

$$\frac{du}{d\tau} = f(\tau, u, p). \quad (3)$$

The generated code is fast and prevents users unfamiliar with Julia or SymBoltz from writing slow code. If necessary, one can escape the standard code generation and call arbitrary numerical functions, for example to solve a nonlinear equation for the minimum of a potential or interpolate tabulated data. The code generation handles tasks like allocating indices for each ODE state u_i , and performs optimizations such as common subexpression elimination (see section 3.2). This is helpful as Boltzmann solvers tend to have big f and ODE solvers call f many times.

2.1.2. Automatic handling of observed variables

A general ODE (3) has two types of variables: “unknowns” $u(\tau)$ are integrated with respect to time, while “observed” variables are any functions of the unknowns. The Einstein-Boltzmann equations are usually written with many observed variables.

For example, consider the metric and gravity equations in appendices A.1 and A.2 sourced by some arbitrary $\rho(\tau)$, $\delta\rho(\tau, k)$ and $\Pi(\tau, k)$. Here $a(\tau)$ and $\Phi(\tau, k)$ are the only unknown (differential) variables that the ODE is solved for, while one can “ob-

serve” $z(\tau)$, $\mathcal{H}(\tau)$, $H(\tau)$ and $\Psi(\tau, k)$ from the unknowns. In addition, observed derivatives like \mathcal{H}' or Ψ' are not always trivial to express, but SymBoltz automatically expands them using the definitions of \mathcal{H} or Ψ . Of course, one can eliminate all observeds by explicitly inserting them into the equations for the unknowns. But this reduces readability, as observed variables are helpful intermediate definitions that break up the equations, and one may want to extract them from the solution as well. Furthermore, modified models can change the sets of unknown and observed variables (e.g. modified gravity can change the constraint equation for Ψ into a differential equation). It is easier to compose models when variables are not hardcoded as either unknown or observed.

SymBoltz reads in a full system of equations like that defined by appendix A and separates variables into unknowns and observeds. It then generates numerical code for solving the ODE for the unknowns (see section 2.1.1), but can automatically recompute any observed variables from the solution of the unknowns.

The bottom line is that users can easily use any variable anywhere by just referring to it, whether it is unknown or observed. In other solvers one may have to look up the expression for observed variables and recompute them manually. This is tedious, error-prone and can tempt users to make simplifying assumptions (e.g. approximating $\Psi \approx \Phi$ without anisotropic stress).

2.1.3. Automatic stage separation and splining of unknowns

In principle, one can solve the Einstein-Boltzmann equations by integrating the entire system (e.g. background and perturbations) at once. However, the system can be broken down into sequential computational stages that each depend only on those before it. To alleviate stiffness in each stage, separate concerns by solving every equation only once (e.g. avoid recomputing the background for every perturbation mode) and to improve performance, all Boltzmann codes solve the system stage-by-stage and spline variables from one stage as input to the next.

To illustrate, again consider the general relativistic equations in appendix A.2 sourced by some known $\rho(\tau)$, $\delta\rho(\tau, k)$ and $\Pi(\tau, k)$. Clearly $\Phi(\tau, k)$ and $\Psi(\tau, k)$ depend on $a(\tau)$, but $a(\tau)$ does not depend on $\Phi(\tau, k)$ or $\Psi(\tau, k)$, reflecting the perturbative nature of the problem. One can first solve for only $a(\tau)$ in the “background”, then spline and look up $a(\tau)$ to solve for $\Phi(\tau, k)$ and $\Psi(\tau, k)$ in the “perturbations”, instead of solving for all three together and repeatedly solve for $a(\tau)$ for every k .

SymBoltz uses the same stage separation strategy as any other Boltzmann code, but automates it with its knowledge of the symbolic equations. First, all equations are split into background and perturbation stages. Cubic Hermite splines are then constructed for all background unknowns (like $a(\tau)$) and passed on to the perturbations. This spline type is optimal for interpolating ODEs, as Hermite splines take both $u(\tau)$ and $u'(\tau)$ into account for better accuracy, and $u'(\tau)$ is known analytically from $u(\tau)$ and definition (3). In contrast, observed variables (like $\mathcal{H}(\tau)$) are computed from the (splined) unknowns because their derivatives are not known directly, and splining them is less accurate. This makes any background variable available in the perturbations “for free”. All stages of the Einstein-Boltzmann equations are solved as if it is written as one combined system of equations, while splining and stage separation are done automatically under the hood.

The separation into background and perturbation stages is guaranteed and just reflects the perturbative structure of the linearized Einstein-Boltzmann equations, where each order depends only on those before it. However, they can often be broken further down: most thermodynamics (recombination) models can be separated from the background, and some variables

⁸ <https://hersle.github.io/SymBoltz.jl/stable/unstructured/>

⁹ Counting `input.{h,c}`, `background.{h,c}`, `thermodynamics.{h,c}`, `perturbations.{h,c}` and `wrap_recfast.{h,c}` with `wc -l`.

have integral solutions (e.g. the optical depth $\kappa(\tau) = \int_{\tau_0}^{\tau} \kappa'(\tilde{\tau}) d\tilde{\tau}$ or line-of-sight integration) that can be computed in isolation after solving the differential equations. In the future, SymBoltz' background-perturbations separation could be extended to automatically split all smaller stages by symbolically inspecting the dependencies between variables in the equations.

2.1.4. Automatic solution interpolation

SymBoltz integrates the background and several perturbation ODEs in conformal time τ for several wavenumbers k . All the results are stored in a special solution object. This solution object can be queried for any variable or symbolic expression

$$S(\tau) \text{ or } S(\tau, k). \quad (4)$$

This looks up the background solution if S is a background variable, or the perturbation solutions if it is perturbative. It interpolates from the times stored by the ODE solver to the requested τ using the solver's dense interpolation. If S is perturbative, it also interpolates from the solved perturbation k -modes to the requested k . If S is an unknown, it is returned directly from the ODE solution. If S is observed, it is instead recomputed automatically from the equation that defines it as a function of the unknowns.

The result is that the user can access any variable in the model without having to do this manually. The solution interpolation is also incorporated into plot recipes for visualization of any variable as a function of τ and/or k .

2.1.5. Automatic Jacobian generation and sparsity detection

Just like SymBoltz generates code for f in the ODE (3), it uses the same symbolic equations to generate its Jacobian \mathbf{J} with entries

$$J_{ij} = \frac{\partial f_i}{\partial u_j}. \quad (5)$$

Jacobians are crucial for solving stiff ODEs with implicit solvers. Manually coding them is tiresome, error-prone, and must be repeated for new models. Numerical evaluation with finite differences is both approximate and slow. It can also be computed with automatic differentiation, but we find this slower and overkill compared to the analytical \mathbf{J} . Analytical Jacobians are as fast and stable as possible, and automatic generation lets the solver benefit from it while the modeler focuses on the high-level equations.

SymBoltz stores the Jacobian in sparse form to boost performance when it has many zeros. From the analytical \mathbf{J} , SymBoltz precomputes its exact sparsity pattern (where $J_{ij} = 0$). This is hard to specify manually, and numerical solvers cannot distinguish false local zeros (for some input) from true global zeros (for all inputs). Without approximations, SymBoltz then reuses the same sparsity structure throughout the integration, computes the nonzero J_{ij} analytically and stores them directly in the sparse \mathbf{J} with no extra cost from looking up sparse matrix indices.

Easy, accurate, fast and sparse Jacobians are crucial for SymBoltz to remain performant without approximations! It is a major advantage with the symbolic approach, as in PyCosmo.

2.2. Approximation-freeness

SymBoltz treats stiffness in the Einstein-Boltzmann equations with modern implicit ODE solvers that integrate the full equations at all times. It is therefore free of approximation schemes, such as the TCA, UFA, RSA, NCDMFA and Saha approximation. This is friendlier to the modeler, who now simply has to

provide a single set of equations instead of deriving approximations, validating them and dealing with related chores. This pairs well with a high-level equation-oriented symbolic interface.

Implicit solvers take more expensive steps than explicit methods. At every step, they solve a generally nonlinear system of equations for the next unknowns \mathbf{u} . Using Newton's method, it iteratively solves linear systems $\mathbf{W}\mathbf{u} = \mathbf{b}$ by LU-factorizing $\mathbf{W} = \mathbf{I} - \gamma h \mathbf{J}$, where γ is a constant, h is the time step and \mathbf{J} is the ODE Jacobian (5).¹⁰ LU-factorizing a dense $n \times n$ matrix from an n -dimensional ODE costs $O(n^3)$ operations and bottlenecks larger ODEs (e.g. larger l_{\max}). In return, implicit methods use more information about the ODE to take stable and long steps.

To be fast, implicit solvers need several optimizations. They must compute not only f , but also \mathbf{J} efficiently. A common trick is to reuse an LU-factorized \mathbf{W} over several steps, even if it really changes. Newton's method only needs an approximate \mathbf{W} to find the root, and \mathbf{W} is recomputed only if convergence is slow due to an outdated \mathbf{J} or a new step size h . This trades fewer LU-factorizations and \mathbf{J} evaluations for more linear solve back-substitutions, which only cost $O(n^2)$ operations. The next trick is to speed up the linear algebra with sparse matrices if \mathbf{W} has many zeros, as for the perturbations. SymBoltz handles this by generating the analytical and sparse Jacobian (see section 2.1.5).

SymBoltz generates code for all implicit solvers in OrdinaryDiffEq.jl¹¹ and dense and sparse matrix methods in LinearSolve.jl¹². We can test different solvers, which is useful as performance and stability of implicit methods and linear algebra operations are problem-dependent. Using $O(100)$ perturbation equations with more than 95% sparsity, we find RFLUFactorization fastest for dense matrices, but KLUFactorization several times faster when exploiting sparsity. We tested these ODE solvers:

– **Backward Differentiation Formula (BDF) methods** like FBDF and QNDF (Shampine & Reichelt 1997) are multi-step methods that use several past points to solve for the next step. They do not have Runge-Kutta “stages” and solve just one implicit equation per step, so they scale well to large ODEs and can reuse Jacobians aggressively. They have variable order of 1-5, but are “L-stable” only up to 2nd order. This makes them take small steps in stiff regimes without utilizing their high order. We find them to be slowest. The solvers ndf15 in CLASS and BDF2 in PyCosmo belong to this family. Nadkarni-Ghosh & Refregier (2017) also discuss BDF methods in the context of the Einstein-Boltzmann equations.

– **Explicit Singly-Diagonal Implicit Runge-Kutta (ES-DIRK) methods** (e.g. Jørgensen et al. 2018) are a class of implicit Runge-Kutta methods designed to preserve most stability properties of Fully Implicit (FIRK) methods at a cheaper computational cost. An s -stage FIRK method has excellent stability, but a dense Butcher tableau a_{ij} and must solve a system of $n \times s$ equations at every step. D in ES-DIRK means that a_{ij} has only lower triangular and diagonal nonzeros, decoupling the system into s systems of n equations that are faster to solve sequentially. S means that all diagonal nonzeros $a_{ii} = \gamma$ are equal, so all stages share the same \mathbf{W} -matrix and only one must be factorized and can be reused as in BDF methods. E means that $a_{11} = 0$, so the first stage is explicit and cheap. Unlike BDF methods, they can remain L-stable without losing order to stiffness. We find the 4th order

¹⁰ For example, the implicit Euler method $\mathbf{u}_{n+1} = \mathbf{u}_n + h f(\tau_{n+1}, \mathbf{u}_{n+1})$ solves $\mathbf{F}(\mathbf{u}_{n+1}) = \mathbf{u}_{n+1} - h f(\tau_{n+1}, \mathbf{u}_{n+1}) - \mathbf{u}_n = \mathbf{0}$ at every step with Newton's method using its Jacobian $\mathbf{W} = \nabla \mathbf{F} = \mathbf{I} - h \mathbf{J}(\tau_{n+1}, \mathbf{u}_{n+1})$.

¹¹ <https://github.com/SciML/OrdinaryDiffEq.jl/>

¹² <https://github.com/SciML/LinearSolve.jl>

KenCarp4 method (Kennedy & Carpenter 2003) to perform well with much fewer time steps. Bolt.jl also defaults to this solver. DISCO-EB uses Kvaerno5, but we find it slower.

– **Rosenbrock methods:** Rosenbrock methods (e.g. Lang 2020) linearize $f \approx Ju$ and effectively replace Newton’s method with one linear solve. Their major upside is being free from convergence on a nonlinear problem. This suits the perturbation ODEs, as they are already linear. The downside is that they can need a new J at every step, which is slow to evaluate numerically in many problems. But generating the Jacobian analytically eliminates this issue. A subclass called “Rosenbrock-W” methods can reuse Jacobians, but this strategy is not yet used by OrdinaryDiffEq.jl. We find the 5th order L-stable Rodas5P method (Steinebach 2023) to be both most efficient and stable on both the background and perturbations, and have not found it used by other Boltzmann codes.

Performance of these methods is compared in section 4.

Traditional codes use approximations to reduce stiffness and increase performance by evolving fewer ODE states when possible. Earlier works find marginal speedups from the TCA and UFA compared to using implicit solvers, but the RSA can significantly speed up models with high l_{\max} (Lesgourges & Tram 2011; Moser et al. 2022; Hahn et al. 2024). However, approximation-based codes must account for the structure of the equations to change, adding overhead to ODE solvers and restructuring sparse Jacobians. Approximation-free solvers can challenge this by optimizing around constant structure. Numerical codes approximate J with finite differences using $O(n)$ evaluations of f . This is wasteful, as $f = Ju$ for linear perturbations and computing the nonzeros of J requires fewer operations than f ! Symbolic codes can take advantage of such properties. Approximations also complicate the code and put more load on modelers to derive, implement and validate them, and repeat the process for modifications that reintroduce stiffness or invalidate approximations.

SymBoltz is tuned for performance without invoking approximations. The approximation-free structure is a major simplification and pairs well with a symbolic high-level equation-oriented interface. In the long run, approximation schemes can of course be explored as a secondary and optional way to maximize speed.

2.3. Differentiability

SymBoltz is compatible with automatic differentiation. It can compute derivatives of any output quantity (e.g. ODE variables, $P(k)$ or C_l) with respect to any input parameters (e.g. h or Ω_{c0}). For example, it can be used to learn the output’s sensitivity to the input, perform Fisher forecasts or compute the Jacobian in the shooting method when parametrizing models with integrated variables. It can also compute the ODE Jacobian, but we do this symbolically to get it analytically with its sparsity pattern.

Currently, SymBoltz and Bolt.jl both work only with forward-mode dual numbers through ForwardDiff.jl¹³. This is appropriate for applications with more outputs than inputs, like differentiating $O(100)$ values of $P(k)$ or C_l as functions of $O(10)$ parameters. Reverse-mode is ideal with fewer outputs and attractive for MCMCs or training emulators where output is compressed to a scalar loss. Fast reverse-mode gradients could accelerate sampling in large parameter spaces from upcoming surveys and challenge use of emulators. Notably, DISCO-EB supports reverse-mode, but has not yet demonstrated it for this purpose. However, reverse-mode in SymBoltz is left for future work.

¹³ <https://github.com/JuliaDiff/ForwardDiff.jl>

3. Examples

The best way to illustrate the features in section 2 is perhaps through some examples. The code is as of SymBoltz version 0.14.1 and available in a notebook in the project repository.

3.1. Basic usage workflow

Most usage follows a model–problem–solution workflow:

```
using SymBoltz
M = ΛCDM(lmax = 16)
p = Dict(
    M.y.T₀ => 2.7, M.b.Ω₀ => 0.05, M.b.YHe => 0.25,
    M.v.Neff => 3.0, M.c.Ω₀ => 0.27, M.h.m_eV => 0.02,
    M.I.ln_As1e10 => 3.0, M.I.ns => 0.96, M.g.h => 0.7
)
prob = CosmologyProblem(M, p; jac=true, sparse=true)
ks = [4, 40, 400, 4000] # k / (H₀/c)
sol = solve(prob, ks)
```

The model–problem–solution split achieves three distinct goals.

First, a purely symbolic representation M of the Λ CDM model is created. This is a standalone object designed to be interactively inspected and modified. It contains every variable, parameter and equation of the cosmological model structured as one submodel per physical component: the metric g , the gravitational theory G , photons γ , massless neutrinos ν , massive neutrinos h , cold dark matter c , baryons b , the cosmological constant Λ and inflation I . For example, `equations(M)` shows all equations; `equations(M.G)` only the gravitational ones; `M.g.a` refers to the scale factor variable $a(\tau)$ that “belongs” to the metric g ; `M.b.Ω₀` is the baryon density parameter Ω_{b0} ; and `parameters(M)` lists parameters that can be set. This displays with L^AT_EX-compatibility in notebooks and transparently shows the equations being solved.

Second, the symbolic model is compiled to a numerical problem `prob` with parameters `p`. This is an expensive step where the processing in section 2.1 happens: equations are checked for consistency and split into background/perturbation stages; observed/unknown variables are distinguished; fast ODE code is generated; background unknowns in the perturbations are replaced by splines; the Jacobian matrix is generated in numerical/analytical and dense/sparse form; and initial values are computed. The compilation is customized with optional arguments like `jac` and `sparse`. This is a separate step because it performs final transformations on the model M once the user has finished modifying and committed to it.

Third, `solve(prob, ks)` solves the background and perturbations for the wavenumbers `ks`. Omitting `ks` solves only the background. The resulting solution object `sol` provides convenient access to all model variables. Internally, it stores values of all ODE unknowns at the time steps taken by the solvers and for every requested wavenumber. But it can be queried with any time, wavenumber and symbolic expression, and will automatically compute it from the unknowns and interpolate between stored times and wavenumbers, as explained in section 2.1.4. For example, calling `sol(1.0, 2.0, g.Φ+g.Ψ)` computes $\Phi + \Psi$ at $k = 1 H_0/c$ and $\tau = 2 H_0^{-1}$ by expanding it in terms of unknowns using the equations in appendix A.2. This interface was used to plot the evolution of several variables in fig. 2 with little code.

Most Boltzmann solvers save only a fixed set of variables, such as only the unknowns. Recovering observed variables requires manual effort. This is cumbersome, opens for user error and adds friction in the modeling process. SymBoltz is designed to provide easy access to all variables defined by the model.

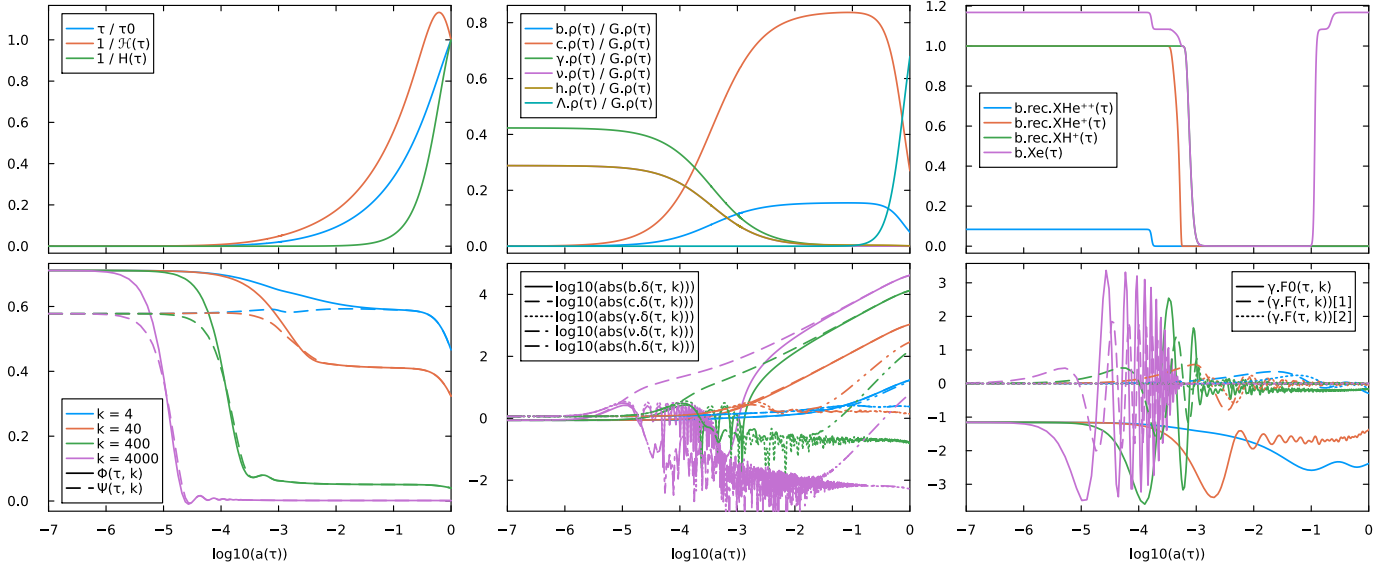


Fig. 2. Included plot recipes in SymBoltz make it trivial to visualize any symbolic variable or expression thereof from a solution of the Einstein-Boltzmann equations. This plot was made with one short line of code per subplot. Wavenumbers k are in units of H_0/c .

3.2. Modifying models

Suppose we want to replace the cosmological constant Λ with another dark energy model, such as dynamical w_0w_a dark energy (Chevallier & Polarski 2001; Linder 2003) with equation of state

$$w(\tau) = w_0 + w_a(1 - a(\tau)). \quad (6)$$

In this case, it is possible to solve the continuity equation

$$\rho'(\tau) = -3\mathcal{H}(\tau)\rho(\tau)(1 + w(\tau)) \quad (7a)$$

analytically with the ansatz $\rho(\tau) \propto a(\tau)^m \exp(na(\tau))$ to get

$$\rho(\tau) = \rho(\tau_0)a(\tau)^{-3(1+w_0+w_a)} \exp(-3w_a(1 - a(\tau))). \quad (7b)$$

Perturbations are given by de Putter et al. (2010). To implement this species in SymBoltz, write down all related variables, parameters, equations and initial conditions in one place:

```

g, tau, k = M.g, M.tau, M.k
a, H, Phi, Psi = g.a, g.H, g.Phi, g.Psi
D = Differential(tau)
@parameters w0 w_a c_s^2 Omega_0 rho0
@variables rho(tau) P(tau) w(tau) c_a^2(tau) delta(tau,k) theta(tau,k) sigma(tau,k)
eqs = [
    w ~ w0 + w_a*(1-a)
    rho0 ~ 3*Omega_0 / (8*Num(pi))
    rho ~ rho0 * a^(-3(1+w0+w_a)) * exp(-3w_a*(1-a))
    P ~ w * rho
    c_a^2 ~ w - 1/(3H) * D(w)/(1+w)
    D(delta) ~ 3H*(w-c_s^2)*delta - (1+w) * (
        (1+9(H/k)^2*(c_s^2-c_a^2))*theta - 3*D(Phi))
    D(theta) ~ (3c_s^2-1)*H*theta + k^2*c_s^2*delta/(1+w) + k^2*Psi
    sigma ~ 0
]
initialization_eqs = [
    delta ~ -3/2 * (1+w) * Psi
    theta ~ 1/2 * (k^2*tau) * Psi
]
X = System(eqns, tau; initialization_eqs, name = :X)

```

Everything is packed down in the w_0w_a component X . Unicode code symbols are encouraged to maximize similarity with equations (e.g. Ω_0 over Omega_0), and SymBoltz will automatically render them in L^AT_EX-compatible environments (e.g. notebooks).

A w_0w_a CDM model is now built by replacing the cosmological constant species Λ in Λ CDM by the w_0w_a species X :

```

M = LambdaCDM(Lambda = X, lmax = 16, name = :w0w_aCDM)
push!(p, X.w0 => -0.9, X.w_a => 0.2, X.c_s^2 => 1.0)
prob = CosmologyProblem(M, p; jac=true, sparse=true)

```

This is all the user has to do. The modification simply consists of writing down the equations verbatim. It could hardly be more compact and to the point. Under the hood, SymBoltz will:

- create input hooks for setting the parameters w_0 , w_a , c_s^2 , Ω_0 ,
- move (τ) -dependent functions to the background,
- move (τ, k) -dependent functions to the perturbations,
- expand $D(w) = dw/d\tau$ and $D(\Phi) = d\Phi/d\tau$ from w and Φ ,
- compute needed background variables in the perturbations,
- spline $\rho(\tau)$ in the perturbations (if we use (7a) over (7b)),
- source gravity with energy-momentum contributions,
- assign $\Omega_{X0} = 1 - \sum_{s \neq X} \Omega_{s0}$ (if gravity is GR) by default,
- eliminate common subexpressions like $x=1+w$ and $y=1/x$,
- generate ODE functions and state indices for δ' and θ' ,
- generate sparse analytical Jacobian entries for δ' and θ' ,
- interpolate and output any variable from the solution, both for unknowns (i.e. δ and θ) and observeds (e.g. w and c_a^2).

Most of these steps require manual intervention in a numerical code. For example, in CLASS one would have to read new parameters in `input.c`; declare new background and perturbation variables in `background.h` and `perturbations.h`; solve background equations, save desired output and source gravity in `background.c`; and recompute or look up background variables, solve perturbation equations, save desired output and source gravity in `perturbations.c`. The changes are scattered across the code, so it grows in complexity as more models are added. SymBoltz opens for a workflow that implements and analyzes a modified model with less effort all in one notebook, for example.

Of course, both codes already include a w_0w_a species, but this is how they are implemented. We proceed with the w_0w_a CDM model.

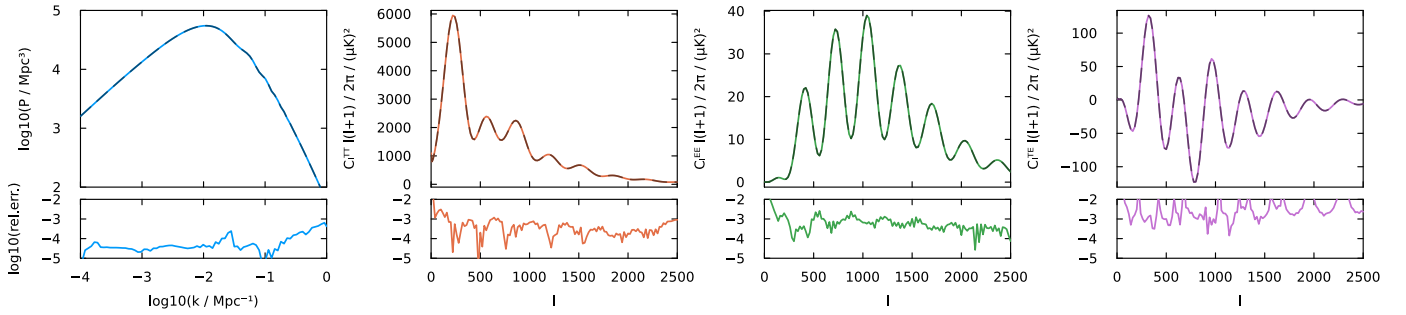


Fig. 3. Matter and CMB (TT, TE and EE) power spectra computed by SymBoltz (SB; colored lines) compared to CLASS (CL; grey dashes) with relative errors $\text{rel.err.} = P_k^{\text{SB}} / P_k^{\text{CL}} - 1$ and $\text{rel.err.} = C_l^{\text{SB}} / C_l^{\text{CL}} - 1$ for the Λ CDM model. CLASS uses the precision parameters in appendix B.

3.3. Computing power spectra

SymBoltz can compute the matter power spectrum $P(k)$ and the angular CMB power spectra C_l^{TT} , C_l^{TE} and C_l^{EE} :

```
ks = 10 .^ range(-1, 4, length = 100)
Ps = spectrum_matter(prob, ks)
ls = vcat([2,3,5,10], 20:20:2500)
jl = SphericalBesselCache(ls)
Cls = spectrum_cmb([:TT, :EE, :TE], prob, jl)
```

The `spectrum_matter` and `spectrum_cmb` functions select a coarse k -grid to solve the perturbations and interpolates to a finer k -grid. This is a common trick to integrate fewer k -modes. Precision parameters that affect the output are given with optional keyword arguments. Output spectra and their computation time with standard precision settings are shown in fig. 3 and table 1.

It shows that SymBoltz and CLASS agree to around 0.1% or better. The $P(k)$ agree to 0.1% for all k and 0.01% for linear k . The C_l agree to 0.1% for most l , but slightly worse for cosmic variance-dominated l and very large l in C_l^{TE} . This is sufficient for most current data (e.g. [Bolliet et al. 2024](#)). It is similar to CAMB vs. CLASS with standard precision, although their agreement is pushed to 0.01% with high precision ([Lesgourgues 2011b](#)).

SymBoltz computes $P(k)$ quickly, but the extra steps needed for C_l are not yet as optimized as they are in CLASS. A more thorough performance comparison for $P(k)$ is given in section 4.

3.4. Differentiable Fisher forecasting

Fisher forecasting is a technique to predict how strong parameter constraints that can be placed by data with given errors. It needs derivatives that can be computed with automatic differentiation.

Near a peak \mathbf{p}_0 , where derivatives vanish, a log-likelihood $\log L$ of parameters \mathbf{p} is approximated by the Taylor series

$$\log L(\mathbf{p}) \approx \log L(\mathbf{p}_0) - \sum_{i,j} F_{ij}(\mathbf{p}_0)(p_i - \bar{p}_i)(p_j - \bar{p}_j), \quad (8)$$

Table 1. Time to compute the power spectra in fig. 3.

| Code (approximations) | $P(k)$ | C_l |
|---|--------|-------|
| SymBoltz (no approximations) | 0.3 s | 3.1 s |
| CLASS (only tight-coupling approximation) | 5.2 s | 8.7 s |
| CLASS (all approximations) | 0.5 s | 1.6 s |

where \mathbf{F} is the Fisher (information) matrix with elements

$$F_{ij}(\mathbf{p}) = -\frac{1}{2} \frac{\partial^2 \log L(\mathbf{p})}{\partial p_i \partial p_j}. \quad (9)$$

Intuitively, \mathbf{F} measures how sharp the peak is, or how sensitive L is in different directions in parameter space. Fisher forecasting is powered by the Cramér-Rao bound $|C_{ij}| \geq |F_{ij}^{-1}|$ for the covariance C_{ij} between parameters p_i and p_j . It is an equality for a Gaussian, for which the likelihood (8) is exact. Thus, inverting $\mathbf{F}(\mathbf{p}_0)$ gives the tightest parameter constraints one can hope for.

To demonstrate differentiable Fisher forecasting with SymBoltz, we make the best possible CMB (TT) measurement: one of \bar{C}_l over the full sky with errors only due to cosmic variance

$$\sigma_l = \sqrt{\frac{2}{2l+1}} \bar{C}_l. \quad (10)$$

Assuming a χ^2 -log-likelihood

$$\log L(\mathbf{p}) = -\frac{1}{2} \sum_l \left(\frac{C_l(\mathbf{p}) - \bar{C}_l}{\sigma_l} \right)^2, \quad (11)$$

the Fisher matrix (9) becomes

$$F_{ij} = \sum_l \frac{\partial C_l}{\partial p_i} \frac{1}{\sigma_l^2} \frac{\partial C_l}{\partial p_j}. \quad (12)$$

The derivatives $\partial C_l / \partial p_i$ are usually found with error-prone finite differences by carefully tuning the step. SymBoltz avoids this problem altogether with automatic differentiation:

```
vary = [
    M.g.h, M.c.Q0, M.b.Q0, M.b.YHe, M.v.Neff,
    M.h.m_eV, M.X.w0, M.X.wa, M.I.ln_As1e10, M.I.ns,
]
genprob = parameter_updater(prob, vary)
jl, ls = SphericalBesselCache(100:25:1000), 100:1000
Cl(p) = spectrum_cmb(:TT, genprob(p), jl, ls)
pe = map(par -> p[par], vary)
dCl_dp = ForwardDiff.jacobian(Cl, pe)
```

Here `vary` orders the parameters to differentiate with respect to, and `genprob` generates a new problem with updated parameters `p`. This prepares a vector-to-vector function `Cl(p)` that is differentiated by `ForwardDiff.jacobian` to compute $\partial C_l / \partial p_i$ with dual numbers, as shown in fig. 4. Computing and inverting the Fisher matrix (12) forecasts the constraints in fig. 5. They are in excellent agreement with finite difference results from CLASS, but these required significant tuning of precision parameters and step sizes.

Differentiable Fisher forecasts have also been done with an Eisenstein-Hu transfer function fit by [Campagne et al. \(2023\)](#), and through an Einstein-Boltzmann solver by [Hahn et al. \(2024\)](#).

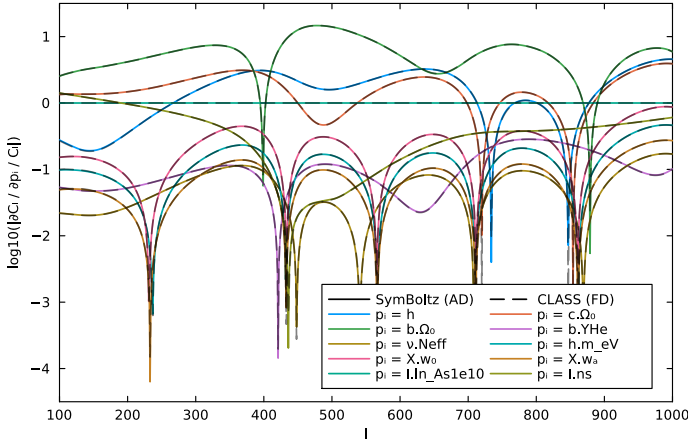


Fig. 4. Normalized derivatives $(\partial C_l / \partial p_i) / C_l$ of a CMB TT power spectrum with respect to cosmological parameters p_i from SymBoltz and automatic differentiation (AD; colored lines) versus CLASS and central finite differences (FD; gray dashes). CLASS uses the precision parameters in appendix B and finite differences with 5% relative step sizes.

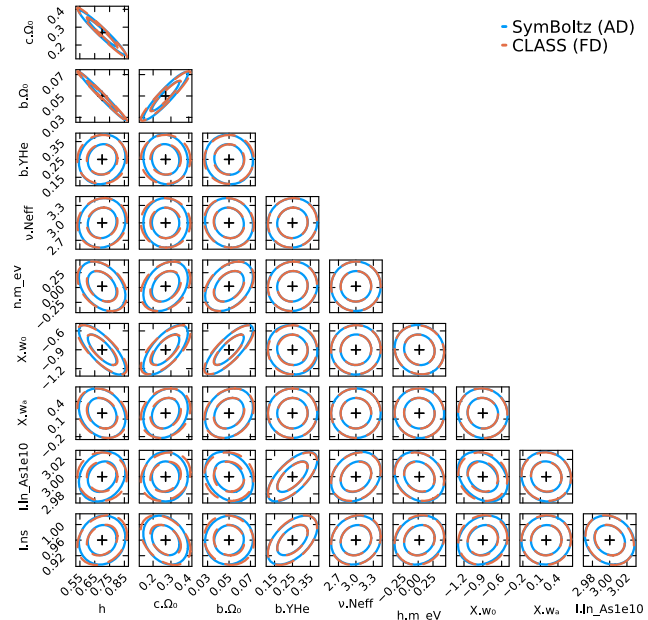


Fig. 5. Marginalized 68% and 95% 2D confidence ellipses for parameter constraints from a Fisher forecast on a cosmic variance-dominated CMB TT-only survey using the derivatives in fig. 4.

3.5. Differentiable MCMC sampling with supernova data

Finally, we show that SymBoltz can output differentiable results for gradient-based MCMC samplers, like the No-U-Turn Sampler (NUTS). It uses gradients to sample parameter space more efficiently than the “blind” Metropolis-Hastings algorithm.

We predict apparent magnitudes $m(z) = M + \mu(z)$ of Type Ia supernovae at redshift z and fit to 1048 Pantheon observations (z_i, m_i) by Scolnic et al. (2018). Their standard absolute magnitude is $M \approx -19.3$, and $\mu(z) = 5 \lg(d_L(z)/10 \text{ pc})$ is the distance modulus from the background-derived luminosity distance¹⁴

$$d_L(z) = \frac{c}{H_0} \frac{\chi(z)}{a(z)} \text{sinc} \left(H_0 \sqrt{-\Omega_{k0}} \chi(z) \right). \quad (13)$$

¹⁴ This expression is valid for any Ω_{k0} with complex $\text{sinc}(x) = \sin(x)/x$, but can be split into branches for positive, negative and zero Ω_{k0} .

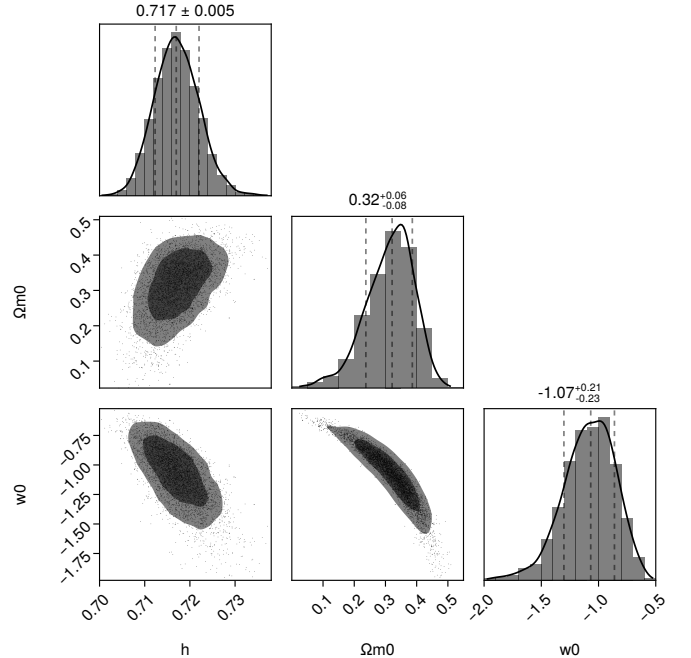


Fig. 6. Parameter inference on 1048 Type Ia supernovae from Pantheon data, using 5000 MCMC samples with the gradient-based NUTS sampler in Turing.jl and differentiable predictions from SymBoltz.

We define the likelihood L by a multivariate normal distribution of the 1048 supernovae with (constant) covariance matrix C given in detail by Scolnic et al. (2018). To compute L , we interface SymBoltz with the probabilistic programming framework Turing.jl (Fjelde et al. 2025), which allows a high-level description of the probabilistic model equivalent to the log-likelihood

$$\log L = -\frac{1}{2} \sum_{i,j} C_{ij}^{-1} (m(z_i) - m_i)(m(z_j) - m_j). \quad (14)$$

We use the NUTS sampler in Turing. The code for this example can be found in the paper’s notebook. For the flat w_0 CDM model ($\Omega_{k0} = 0$, $w_a = 0$, fixed Ω_{r0}) it gives the constraints in fig. 6.

The differentiable computation is not yet fast enough for MCMCs with perturbation-derived spectra. The results here are not groundbreaking, but show that the differentiable pipeline is functional. This is a first step to differentiating the solver quickly, and we aim to accelerate this computation with future work.

Differentiable Boltzmann codes have yet to demonstrate this ability, but more advanced MCMCs with a differentiable background have been done by Campagne et al. (2023), for example.

4. Performance comparison to CLASS

Figure 7 compares performance versus precision of the matter power spectrum $P(k)$ computed with SymBoltz and CLASS. This computation solves the background, thermodynamics and perturbations for several k and reads off $P(k)$ at the final time. The work is dominated by the perturbations, so it is a relevant test of SymBoltz’ approximation-free treatment of perturbations.

The comparison shows how approximations and the ODE solver affect integration of the Einstein-Boltzmann equations. Without approximations, SymBoltz with Rodas5P is more than 10× faster than CLASS with its implicit ndf15 evolver at comparable precision. When CLASS uses approximations and explicit evolver, SymBoltz is as fast while remaining approximation-free.

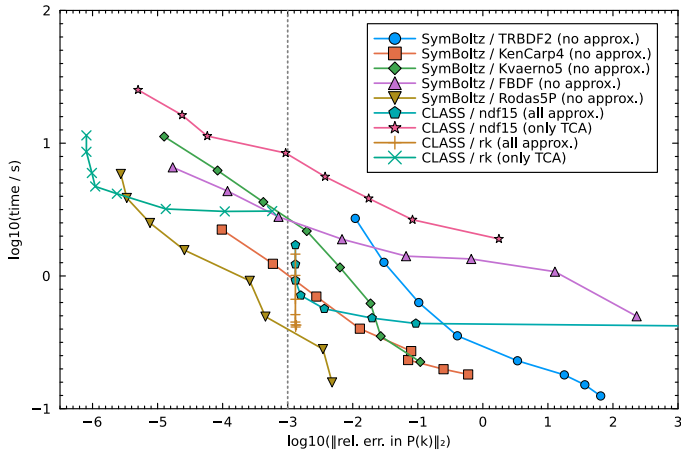


Fig. 7. Work vs. precision for computing the matter power spectrum $P(k)$ with SymBoltz and CLASS. SymBoltz is approximation-free and run with several implicit ODE solvers. CLASS is run with approximations on/off, its implicit/explicit evolvers $ndf15/rk$ and precision settings in appendix B, but tight coupling is always approximated. For each setup, $P(k)$ is computed by integrating perturbation k -modes with ODE solver tolerances 10^{-2} – 10^{-9} that controls the adaptive stepping. For each tolerance, we record the best of 3 runtimes and the L_2 -compressed error $(\sum_{i=1}^N (P(k_i)/\bar{P}(k_i) - 1)^2/N)^{1/2}$ relative to high-precision spectra $\bar{P}(k)$ from both codes with approximations off, tolerance 10^{-10} and FBDF/ndf15. Both codes solve a w_0w_a CDM model with equal parameters, $N = 114$ equal wavenumbers k_i , multipole cutoff $l_{\max} = 16$ for all species, default sampling of massive neutrino momenta and parallelize over k . Times are from a Linux laptop with Intel i7-12800H CPU.

To make this comparison as fair as possible, we configured both codes to integrate identical k -modes (decided by CLASS) without k -interpolation and use the same multipole cutoff l_{\max} for all species. However, the codes sample massive neutrino momenta q differently. This greatly impacts the number of perturbation equations (see appendix A.7). SymBoltz' 4 default momenta gives 127 perturbation equations in total. CLASS' default `tol_ncdm_newtonian = 10-5` gives 11 momenta and 245 equations (before approximations). Increasing this tolerance to 10^{-3} gives 5 momentum bins, 143 equations and is around $245/143 \approx 1.7$ times faster, but introduces errors beyond 1% in $P(k)$. We therefore leave both codes with default q -sampling, but note that CLASS could be up to 2 \times faster at unchanged precision with sparser sampling. This would shift its curves down by $\lg 2 \approx 0.3$. Howlett et al. (2012) (in appendix A) also find a precise 3–4 point scheme in CAMB, and Lee et al. (2025) speed up CLASS using integral equations for massive neutrinos in the fork CLASSIER.

Despite lack of approximation schemes, SymBoltz is fast due to high-order implicit solvers like Rodas5P that take accurate and long steps, fast functions for f and the analytically generated \mathbf{J} , sparse matrix methods with a constant predetermined sparsity structure and efficient sampling of massive neutrino momenta.

SymBoltz is currently slower than CAMB and CLASS for computing C_l . This is subject to more optimizations than $P(k)$, such as sampling of the source function $S(\tau, k)$, interpolation in τ , k , and l , evaluation of spherical Bessel functions $j_l(x)$ and optimized line-of-sight quadrature. These are very well polished by CAMB and CLASS, and unmatched by SymBoltz at this time. A detailed performance analysis for C_l is therefore not meaningful now (but see table 1). With more work, the C_l optimizations can be added to SymBoltz. The purpose of the comparison made here is to show the viability of approximation-free perturbations, which was a major milestone in designing SymBoltz.

5. Future work

We hope SymBoltz continues to grow and that others can build on it. Its symbolic capabilities can be extended with utilities for:

- separation into finer computational stages (see section 2.1.3);
- gauge transformation of equations (e.g. Newtonian \leftrightarrow synchronous gauge), as already possible in CAMB¹⁵;
- perturbation theory utilities for deriving initial conditions and approximation schemes for new models;
- transformation of differential equations with respect to conformal time τ to another (one-to-one) independent variable (e.g. to get observables as direct functions of redshift z);
- validation of dimensions in symbolic equations to catch modeling mistakes by tagging variables with physical units;
- symbolic tensor manipulation to aid work with modified gravity theories (as a standalone package).

These tasks traditionally involve manual error-prone calculations, so such utilities could ease exploration of extended models.

We particularly aim to improve performance for differentiable runs to the level of standard runs. An attractive milestone is fast reverse-mode gradients of scalar loss functions for gradient-based MCMCs. We anticipate the symbolic structure and Jacobian generation to be useful for this, as writing $\mathbf{u}(\tau, \mathbf{p})$ in the ODE (3) and differentiating it for $\mathbf{v}_i = \partial \mathbf{u} / \partial p_i$ gives $d\mathbf{v}_i / d\tau = \mathbf{J}\mathbf{v}_i + \partial f / \partial p_i$, which could be constructed analytically.

It is left for future work to generalize the code from scalar to vector and tensor perturbations, from flat to curved spacetimes, and from adiabatic to other initial conditions. Some additional models like quintessence dark energy and Brans-Dicke gravity are in the works, and we invite others to add extended models.

We hope SymBoltz can foster growth of modular interoperating packages for cosmology in Julia. For example, applications like higher-order perturbation theory (e.g. CLASS-PT by Chudaykin et al. (2020) and PyBird by D'Amico et al. (2021)), nonlinear boosting (e.g. HALOFIT by Takahashi et al. (2012) and HMCODE by Mead et al. (2021)), CMB lensing (e.g. CMBLensing.jl by Millea et al. (2020)) and nonlinear N -body simulations all rely on output from Boltzmann solvers. Supporting automatic differentiation across language barriers is hard, and an ecosystem of such packages in one language with support for automatic differentiation, like Julia or Python with JAX, could create a modular and differentiable cosmological modeling toolbox. A recent example of this is DISCO-DJ's coupling of differentiable Boltzmann and N -body codes for end-to-end modeling from linear perturbations to non-linear structure formation (Hahn et al. 2024; List et al. 2025).

6. Conclusion

SymBoltz is a fresh Julia package for solving the linear Einstein-Boltzmann equations. It features a symbolic-numeric interface where models are built from symbolic equations and compiled to efficient numerical code. This lets modelers prototype new models with few lines code at a high level. It relaxes all approximation schemes found in older codes by solving a single set of stiff equations at all times with implicit integrators. This simplifies the equations and remains performant due to high-order implicit solvers with fast generated code for ODEs and analytical and sparse Jacobians. It is differentiable, so one can get accurate derivatives of any output quantity with respect to any input parameter. Output power spectra agree with CLASS to 0.1% with standard precision and can be used fit to current data.

¹⁵ <https://camb.readthedocs.io/en/latest/symbolic.html>

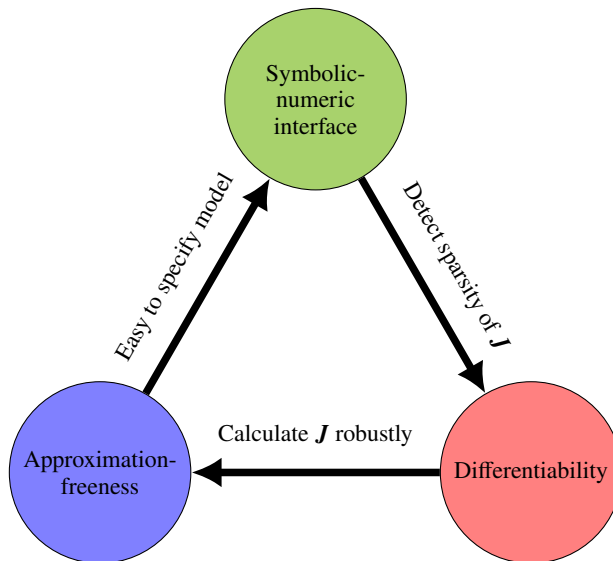


Fig. 8. A symbolic-numeric interface, approximation-freeness and differentiability are three main features of SymBoltz that form a synergy. Differentiability computes the ODE Jacobian J accurately and efficiently; which is used by implicit solvers to integrate stiff ODEs without approximations; which makes it easier to write down equations in simple symbolic form; which is used to find the sparsity pattern of J ; which speeds up J and the implicit solver. This is a self-reinforcing design.

Other recent codes like PyCosmo, Bolt.jl and DISCO-EB also incorporate some of these features. SymBoltz combines them and reinforces its design with a synergy between them, as explained in fig. 8. Together, these new codes offer a simpler alternative in high-level languages that complements traditional codes like CAMB and CLASS that are historically highly tuned around approximations in low-level languages. However, new codes need more work to reach the level of features and maturity of CAMB and CLASS that have grown over many years.

SymBoltz version 0.14.1 includes the flat Newtonian gauge metric, General Relativity, cold dark matter, photons, baryons and RECFAST recombination, massless and massive neutrinos, the cosmological constant and $w_0 w_a$ dark energy with scalar perturbations, distances and matter and CMB spectra. Forward-mode automatic differentiation works for single-run purposes like Fisher forecasting. Fast reverse-mode scalar loss gradients, particularly through the perturbations, is a future milestone that could challenge emulators in gradient-based MCMC sampling. No differentiable Boltzmann code is yet capable of this.

SymBoltz is easy to install from <https://github.com/hersle/SymBoltz.jl>. Documentation¹⁶ is available, and the code is tested with continuous integration to remain correct and up-to-date (see appendix C). All questions and contributions are welcome in the repository! We hope SymBoltz proves useful and that it offers valuable ideas on the Boltzmann solver market.

Acknowledgments

I thank the Julia community for creating an open ecosystem of scientific packages underlying SymBoltz. I thank Aayush Sabharwal and Christopher Rackauckas for developing Modeling-Toolkit.jl and OrdinaryDiffEq.jl and answering questions. I thank Hans A. Winther for helpful suggestions and feedback on the code and drafts of this paper. I thank Julien Lesgourgues, Thomas Tram and others for developing and documenting CLASS.

¹⁶ <https://hersle.github.io/SymBoltz.jl/>

References

Bezanson, J., Edelman, A., Karpinski, S., & Shah, V. B. 2017, SIAM Rev., 59, 65 [[arXiv:1411.1607](https://arxiv.org/abs/1411.1607)]

Blas, D., Lesgourgues, J., & Tram, T. 2011, JCAP, 07, 034 [[arXiv:1104.2933](https://arxiv.org/abs/1104.2933)]

Bolliet, B., Spurio Mancini, A., Hill, J. C., et al. 2024, MNRAS, 531, 1351 [[arXiv:2303.01591](https://arxiv.org/abs/2303.01591)]

Bonici, M., Bianchini, F., & Ruiz-Zapatero, J. 2024, TheOJA, 7 [[arXiv:2307.14339](https://arxiv.org/abs/2307.14339)]

Bull, P., Akrami, Y., Adamek, J., et al. 2016, Physics of the Dark Universe, 12, 56 [[arXiv:1512.05356](https://arxiv.org/abs/1512.05356)]

Campagne, J.-E., Lanusse, F., Zuntz, J., et al. 2023, TheOJA, 6 [[arXiv:2302.05163](https://arxiv.org/abs/2302.05163)]

Casas, S., Fidler, C., Bolliet, B., Villaescusa-Navarro, F., & Lesgourgues, J. 2025, ArXiv [[arXiv:2508.05728](https://arxiv.org/abs/2508.05728)]

Chevallier, M. & Polarski, D. 2001, Int. J. Mod. Phys. D, 10, 213 [[arXiv:gr-qc/0009008](https://arxiv.org/abs/gr-qc/0009008)]

Chudaykin, A., Ivanov, M. M., Philcox, O. H. E., & Simonović, M. 2020, Phys. Rev. D, 102, 063533 [[arXiv:2004.10607](https://arxiv.org/abs/2004.10607)]

D'Amico, G., Senatore, L., & Zhang, P. 2021, JCAP, 2021, 006 [[arXiv:2003.07956](https://arxiv.org/abs/2003.07956)]

de Putter, R., Huterer, D., & Linder, E. V. 2010, Phys. Rev. D, 81, 103513 [[arXiv:1002.1311](https://arxiv.org/abs/1002.1311)]

DESI Collaboration. 2016, ArXiv [[arXiv:1611.00036](https://arxiv.org/abs/1611.00036)]

Dewdney, P. E., Hall, P. J., Schilizzi, R. T., & Lazio, T. J. L. W. 2009, Proc. IEEE, 97, 1482 [[DOI:10.1109/JPROC.2009.2021005](https://doi.org/10.1109/JPROC.2009.2021005)]

Doran, M. 2005a, JCAP, 10, 011 [[arXiv:astro-ph/0302138](https://arxiv.org/abs/astro-ph/0302138)]

Doran, M. 2005b, JCAP, 06, 011 [[arXiv:astro-ph/0503277](https://arxiv.org/abs/astro-ph/0503277)]

Ekanathan, S., Smith, O., & Rackauckas, C. 2025, ArXiv [[arXiv:2412.14362](https://arxiv.org/abs/2412.14362)]

Euclid Collaboration. 2025, A&A, 697, A1 [[arXiv:2405.13491](https://arxiv.org/abs/2405.13491)]

Fjeldé, T. E., Xu, K., Widmann, D., et al. 2025, ACM Trans. Probab. Mach. Learn., 1, 1 [[DOI:10.1145/3711897](https://doi.org/10.1145/3711897)]

Freedman, W. L. 2017, Nat Astron, 1, 0121 [[arXiv:1706.02739](https://arxiv.org/abs/1706.02739)]

Gowda, S., Ma, Y., Cheli, A., et al. 2022, ArXiv [[arXiv:2105.03949](https://arxiv.org/abs/2105.03949)]

Hahn, O., List, F., & Porqueres, N. 2024, JCAP, 06, 063 [[arXiv:2311.03291](https://arxiv.org/abs/2311.03291)]

Hastings, W. K. 1970, Biometrika, 57, 97 [[DOI:10.1093/biomet/57.1.97](https://doi.org/10.1093/biomet/57.1.97)]

Hoffman, M. D. & Gelman, A. 2011, ArXiv [[arXiv:1111.4246](https://arxiv.org/abs/1111.4246)]

Howlett, C., Lewis, A., Hall, A., & Challinor, A. 2012, JCAP, 2012, 027 [[arXiv:1201.3654](https://arxiv.org/abs/1201.3654)]

Jørgensen, J. B., Kristensen, M. R., & Thomsen, P. G. 2018, ArXiv [[arXiv:1803.01613](https://arxiv.org/abs/1803.01613)]

Kennedy, C. A. & Carpenter, M. H. 2003, Applied Numerical Mathematics, 44, 139 [[DOI:10.1016/S0168-9274\(02\)00138-1](https://doi.org/10.1016/S0168-9274(02)00138-1)]

Lang, J. 2020, ArXiv [[arXiv:2002.12028](https://arxiv.org/abs/2002.12028)]

Lee, N., Bernal, J. L., Günther, S., Ji, L., & Kamionkowski, M. 2025, Phys. Rev. D, 112, 043529 [[arXiv:2506.01956](https://arxiv.org/abs/2506.01956)]

Lesgourgues, J. 2011a, ArXiv [[arXiv:1104.2932](https://arxiv.org/abs/1104.2932)]

Lesgourgues, J. 2011b, ArXiv [[arXiv:1104.2934](https://arxiv.org/abs/1104.2934)]

Lesgourgues, J. & Tram, T. 2011, JCAP, 09, 032 [[arXiv:1104.2935](https://arxiv.org/abs/1104.2935)]

Lewis, A. 2025, CAMB Notes [<https://cosmologist.info/notes/CAMB.pdf>]

Lewis, A., Challinor, A., & Lasenby, A. 2000, ApJ, 538, 473 [[arXiv:astro-ph/9911177](https://arxiv.org/abs/astro-ph/9911177)]

Li, Z., Sullivan, J., & Millea, M. 2023 [[DOI:10.5281/zenodo.10065126](https://doi.org/10.5281/zenodo.10065126)]

Linder, E. V. 2003, Phys. Rev. Lett., 90, 091301 [[arXiv:astro-ph/0208512](https://arxiv.org/abs/astro-ph/0208512)]

List, F., Hahn, O., Flöss, T., & Winkler, L. 2025, ArXiv [[arXiv:2510.05206](https://arxiv.org/abs/2510.05206)]

LSST Science Collaboration. 2009, ArXiv [[arXiv:0912.0201](https://arxiv.org/abs/0912.0201)]

Ma, C.-P. & Bertschinger, E. 1995, ApJ, 455, 7 [[arXiv:astro-ph/9506072](https://arxiv.org/abs/astro-ph/9506072)]

Ma, Y., Gowda, S., Anantharaman, R., et al. 2022, ArXiv [[arXiv:2103.05244](https://arxiv.org/abs/2103.05244)]

Mead, A., Brienden, S., Tröster, T., & Heymans, C. 2021, MNRAS, 502, 1401 [[arXiv:2009.01858](https://arxiv.org/abs/2009.01858)]

Millea, M., Anderes, E., & Wandelt, B. D. 2020, Phys. Rev. D, 102, 123542 [[arXiv:2002.00965](https://arxiv.org/abs/2002.00965)]

Moser, B., Lorenz, C. S., Schmitt, U., et al. 2022, Astronomy and Computing, 40, 100603 [[arXiv:2112.08395](https://arxiv.org/abs/2112.08395)]

Nadkarni-Ghosh, S. & Refregier, A. 2017, MNRAS, 471, 2391 [[arXiv:1612.06697](https://arxiv.org/abs/1612.06697)]

Peebles, P. J. E. & Yu, J. T. 1970, ApJ, 162, 815 [[DOI:10.1086/150713](https://doi.org/10.1086/150713)]

Piras, D., Polanska, A., Mancini, A. S., Price, M. A., & McEwen, J. D. 2024, TheOJA, 7 [[arXiv:2405.12965](https://arxiv.org/abs/2405.12965)]

Rackauckas, C. & Nie, Q. 2017, JÖRS, 5, 1 [[DOI:10.5334/jors.151](https://doi.org/10.5334/jors.151)]

Refregier, A., Gamper, L., Amara, A., & Heisenberg, L. 2018, Astronomy and Computing, 25, 38 [[arXiv:1708.05177](https://arxiv.org/abs/1708.05177)]

Revels, J., Lubin, M., & Papamarkou, T. 2016, ArXiv [[arXiv:1607.07892](https://arxiv.org/abs/1607.07892)]

Scolnic, D. M., Jones, D. O., Rest, A., et al. 2018, ApJ, 859, 101 [[arXiv:1710.00845](https://arxiv.org/abs/1710.00845)]

Scott, D. & Moss, A. 2009, MNRAS, 397, 445 [[arXiv:0902.3438](https://arxiv.org/abs/0902.3438)]

Seager, S., Sasselov, D. D., & Scott, D. 1999, ApJ, 523, L1 [[arXiv:astro-ph/9909275](https://arxiv.org/abs/astro-ph/9909275)]

Seljak, U., Aslanyan, G., Feng, Y., & Modi, C. 2017, JCAP, 12, 009 [[arXiv:1706.06645](https://arxiv.org/abs/1706.06645)]

Seljak, U. & Zaldarriaga, M. 1996, ApJ, 469, 437 [[arXiv:astro-ph/9603033](https://arxiv.org/abs/astro-ph/9603033)]

Shampine, L. F. & Reichelt, M. W. 1997, SIAM J. Sci. Comput., 18, 1 [[DOI:10.1137/S1064827594276424](https://doi.org/10.1137/S1064827594276424)]

Steinebach, G. 2023, BIT, 63, 27 [[DOI:10.1007/s10543-023-00967-x](https://doi.org/10.1007/s10543-023-00967-x)]

The Simons Observatory Collaboration. 2019, JCAP, 02, 056 [[arXiv:1808.07445](https://arxiv.org/abs/1808.07445)]

Wong, W. Y., Moss, A., & Scott, D. 2008, MNRAS, 386, 1023 [[arXiv:0711.1357](https://arxiv.org/abs/0711.1357)]

Appendix A: List of equations and practical implementation details

This appendix summarizes the equations that define the standard Λ CDM model in SymBoltz and comments on their practical implementation. We hope this can be a useful reference for others. The list is structured like SymBoltz with one component per subsection. Variables are in units where “ $G = c = H_0 = 1$ ” and temperatures are in K, unless otherwise is stated. These units are chosen because G , c and H_0 can be divided out from the Einstein equations as natural units, but this requires some conversion in the recombination equations that depend explicitly on H_0 . In other words, times are in units of $1/H_0$, distances in c/H_0 and masses in c^3/H_0G . When G , c or and H_0 appear explicitly in the equations, they are in SI units and used only to convert from SI units into the dimensionless units. The equations closely follow the conventions in the seminal paper by [Ma & Bertschinger \(1995\)](#) and very closely matches the source code of SymBoltz with Unicode characters. It is far outside the scope of this paper to derive the equations and explain the meaning of every variable.

The independent variable is conformal time τ , and all derivatives $' = d/d\tau$ are with respect to it (in units of $1/H_0$). This is perhaps the most common parametrization in the literature, and is natural because most equations are autonomous with respect to τ (i.e. $f(\tau, \mathbf{u}) \rightarrow f(\mathbf{u})$, except some multipole truncation schemes that use $1/(k\tau)$, but these are unphysical). By default, integration starts from the early time $\tau = \tau_i = 10^{-6}$, and is terminated when the scale factor crosses $a = 1$, and the corresponding time $\tau = \tau_0$ is labeled today.

A.1. Metric and spacetime (g)

SymBoltz is currently only formulated in the conformal Newtonian gauge, with this metric and related quantities:

$$g_{0i} = g_{i0} = -a^2(1 + 2\Psi)\delta_{0i}, \quad g_{ij} = a^2(1 - 2\Phi)\delta_{ij}, \quad z = \frac{1}{a} - 1, \quad \mathcal{H} = \frac{a'}{a}, \quad H = \frac{\mathcal{H}}{a}, \quad \chi = \tau_0 - \tau.$$

Here \mathcal{H} and H are the conformal and cosmic Hubble factors (in units where $\mathcal{H}_0 = H_0 = 1$). The scale factor a is related to redshift z , and χ is the lookback time from today that appears in some integral solutions. SymBoltz is currently restricted to a flat spacetime.

A.2. General relativity (G)

The gravitational theory of the Λ CDM model is General Relativity governed by the Einstein field equations $G_{\mu\nu} = 8\pi T_{\mu\nu}$. By default, SymBoltz solves for the metric variables a , Φ and Ψ with $(\mu, \nu) = (0, 0)$ in the background (1st Friedmann equation) and $(\mu, \nu) = \{(0, 0), (i, j)\}$ in the perturbations:

$$a' = \sqrt{\frac{8\pi}{3}\rho}a^2, \quad \Phi' = -\mathcal{H}\Psi - \frac{k^2}{3\mathcal{H}}\Phi - \frac{4\pi}{3}\frac{a^2}{\mathcal{H}}\delta\rho, \quad \Psi = -\Phi - 12\pi\left(\frac{a}{k}\right)^2\Pi.$$

Note that it is also possible to evolve other redundant combinations of the Einstein equations (such as the acceleration equation). The equations are coupled to total densities ρ , $\delta\rho$, pressures P and anisotropic stresses Π for an arbitrary set of species s that are present in the cosmological model:

$$\rho = \sum_s \rho_s, \quad P = \sum_s P_s, \quad \delta\rho = \sum_s \delta\rho_s = \sum_s \delta_s \rho_s, \quad \delta P = \sum_s \delta P_s = \sum_s \delta_s \rho_s c_{s,s}^2, \quad \Pi = \sum_s \Pi_s = \sum_s (\rho_s + P_s)\sigma_s.$$

We emphasize that the gravity component is completely unaware of all particle species and makes no assumptions about them. It only reacts to total stress-energy components. All species must therefore define ρ , P , $\delta\rho$, δP and Π explicitly, even if zero. This requirement is somewhat pedantic, but helps isolate components from each other for greater reuse when composing models.

The scale factor a is initialized as the nonlinear solution of the Friedmann equation constrained to $\mathcal{H} = 1/\tau$ (motivated by its radiation-dominated solution $a = \sqrt{\Omega_{r0}}\tau$). The constraint potential is initialized to $\Psi = 20C/(15 + 4f_\nu)$ with the (arbitrary) integration constant $C = 1/2$ and initial energy density fraction $f_\nu = (\rho_\nu + \rho_h)/(\rho_\nu + \rho_h + \rho_\gamma)$ of all (massless and massive) neutrino species relative to all species that are radiative at early times. The evolved potential Φ is initialized accordingly from the constraint equation (the found solution is close to $\Phi = (1 + 2f_\nu/5)\Psi$, but providing both Φ and Ψ explicitly leads to overdetermined initialization equations due to the constraint equation).

The next sections present the Λ CDM section of the “library of species” that are available in SymBoltz.

A.3. Cold dark matter (c)

Cold dark matter is a non-relativistic and non-interacting species that follows very simple equations:

$$w = 0, \quad c_s^2 = w, \quad P = 0, \quad \rho = \frac{\rho_0}{a^3}, \quad \delta' = -\theta + 3\Phi', \quad \theta' = -\mathcal{H}\theta + k^2\Psi, \quad u = \frac{\theta}{k}, \quad \sigma = 0.$$

Initial conditions are adiabatic with $\delta/(1 + w) = -3\Psi/2$ and $\theta = k^2\tau\Psi/2$. The species is parametrized by the reduced density $\Omega_0 = \frac{8\pi}{3}\rho_0$ today.

A.4. Baryons (b)

Baryons are also non-relativistic, but interact with photons through Compton scattering and are subject to recombination physics. This significantly complicates their behavior. SymBoltz currently implements equations from RECFAST¹⁷ version 1.5.2 (Seager et al. 1999; Wong et al. 2008; Scott & Moss 2009):

$$\begin{aligned}
w &= 0, & P &= 0, & \rho &= \frac{\rho_0}{a^3}, & f_{\text{He}} &= \frac{Y_{\text{He}}}{\frac{m_{\text{He}}}{m_{\text{H}}}(1 - Y_{\text{He}})}, & n_{\text{H}} &= \frac{(1 - Y_{\text{He}})\rho}{m_{\text{H}}}, & n_{\text{He}} &= f_{\text{He}}n_{\text{H}}, & c_s^2 &= \frac{k_B}{\mu c^2} \left(T_b - \frac{T'_b}{3\mathcal{H}} \right), \\
\beta &= \frac{1}{k_B T_b}, & T'_b &= -2\mathcal{H}T_b - \frac{a}{H_0} \frac{8}{3} \frac{T_\gamma^4 X_{\text{e}}}{1 + f_{\text{He}} + X_{\text{e}}}(T_b - T_\gamma), & \mu &= \frac{m_{\text{H}}}{1 + (\frac{m_{\text{H}}}{m_{\text{He}}}) - 1} \frac{Y_{\text{He}}}{Y_{\text{He}} + (1 - Y_{\text{He}})X_{\text{e}}}, & \kappa' &= -\frac{a}{H_0} n_{\text{e}} \sigma_{TC}, \\
v &= -\kappa' e^{-\kappa}, & n_{\text{e}} &= X_{\text{e}} n_{\text{H}}, & X_{\text{e}} &= X_{\text{H}}^+ + X_{\text{He}}^{++} + f_{\text{He}} X_{\text{He}}^+ + X_{\text{e}}^{\text{re1}} + X_{\text{e}}^{\text{re2}}, & X_{\text{H}}^{+'} &= -\frac{a}{H_0} C_{\text{H}} \left(\alpha_{\text{H}} n_{\text{e}} X_{\text{H}}^+ - \beta_{\text{H}} e^{-\beta_b E_{\text{H}}^{2s,1s}} (1 - X_{\text{H}}^+) \right), \\
X_{\text{He1}}^{+'} &= -\frac{a}{H_0} C_{\text{He1}} \left(\alpha_{\text{He1}} n_{\text{e}} X_{\text{He}}^+ - \beta_{\text{He1}} e^{-\beta_b E_{\text{He1}}^{2s,1s}} (1 - X_{\text{He}}^+) \right), & X_{\text{He3}}^{+'} &= -\frac{a}{H_0} C_{\text{He3}} \left(n_{\text{e}} \alpha_{\text{He3}} X_{\text{He}}^+ - 3\beta_{\text{He3}} e^{-\beta_b E_{\text{He3}}^{2s,1s}} (1 - X_{\text{He}}^+) \right), \\
X_{\text{He}}^{+'} &= X_{\text{He1}}^{+'} + X_{\text{He3}}^{+'}, & X_{\text{He}}^{++} &= \frac{2f_{\text{He}} R_{\text{He}}^+}{\left(1 + f_{\text{He}} + R_{\text{He}}^+ \right) \left(1 + \sqrt{1 + \frac{4f_{\text{He}} R_{\text{He}}^+}{(1 + f_{\text{He}} + R_{\text{He}}^+)^2}} \right)}, & R_{\text{He}^+} &= \frac{\exp(-\beta E_{\text{He}^+}^{\infty,1s})}{n_{\text{H}} \lambda_{\text{e}}^3}, & \lambda_{\text{e}} &= \frac{h}{\sqrt{2\pi m_{\text{e}}/\beta}}, \\
X_{\text{e}}^{\text{re1}} &= \frac{1 + f_{\text{He}}}{2} + \frac{1 + f_{\text{He}}}{2} \tanh \left(\frac{4}{3} \frac{(1 + z^{\text{re1}})^{3/2} - (1 + z)^{3/2}}{(1 + z^{\text{re1}})^{1/2}} \right), & X_{\text{e}}^{\text{re2}} &= \frac{f_{\text{He}}}{2} + \frac{f_{\text{He}}}{2} \tanh \left(\frac{4}{3} \frac{(1 + z^{\text{re2}})^{3/2} - (1 + z)^{3/2}}{(1 + z^{\text{re2}})^{1/2}} \right), \\
\delta' &= -\theta - 3\mathcal{H}c_s^2\delta + 3\Phi', & \theta' &= -\mathcal{H}\theta + k^2 c_s^2 \delta + k^2 \Psi - \frac{4}{3} \kappa' \frac{\rho_\gamma}{\rho_b} (\theta_\gamma - \theta_b), & u &= \frac{\theta}{k}, & \sigma &= 0.
\end{aligned}$$

Transition rates and coefficients related to recombination of Hydrogen include fitting functions that emulate the results of more accurate and expensive computations (here $\ln(a)$ is the logarithm of the scale factor, while (Fa) is an unrelated fudge factor):

$$\begin{aligned}
\alpha_{\text{H}} &= 10^{-19} (Fa) \frac{\left(\frac{T_b}{T_0} \right)^b}{1 + c \left(\frac{T_b}{T_0} \right)^d}, & \beta_{\text{H}} &= \frac{\alpha_{\text{H}}}{\lambda_{\text{e}}^3} \exp(-\beta E_{\text{H}}^{\infty,2s}), \\
K_{\text{H}} &= \left(1 + A_1 \exp \left(-\left(\frac{\ln(a) - \ln(a_1)}{w_1} \right)^2 \right) + A_2 \exp \left(-\left(\frac{\ln(a) - \ln(a_2)}{w_2} \right)^2 \right) \right) \frac{(\lambda_{\text{H}}^{2s,1s})^3}{8\pi H}, & C_{\text{H}} &= \frac{1 + K_{\text{H}} \Lambda_{\text{H}} n_{\text{H}} (1 - X_{\text{H}}^+)}{1 + K_{\text{H}} (\Lambda_{\text{H}} + \beta_{\text{H}}) n_{\text{H}} (1 - X_{\text{H}}^+)}.
\end{aligned}$$

Helium rates and coefficients are even more complicated. First, Helium includes contributions from singlet states (He_1):

$$\begin{aligned}
\alpha_{\text{He1}} &= \frac{q_1}{\sqrt{\frac{T_b}{T_2}} \left(1 + \sqrt{\frac{T_b}{T_2}} \right)^{1-p_1} \left(1 + \sqrt{\frac{T_b}{T_1}} \right)^{1+p_1}}, & \beta_{\text{He1}} &= 4 \frac{\alpha_{\text{He1}}}{\lambda_{\text{e}}^3} \exp(-\beta E_{\text{He1}}^{\infty,2s}), & K_{\text{He1}} &= \frac{1}{K_{\text{He1}}^{-1} + K_{\text{He1}}^{-1} + K_{\text{He1}}^{-1}}, \\
K_{\text{He1}}^{-1} &= \frac{8\pi H}{(\lambda_{\text{He1}}^{2p,1s})^3}, & K_{\text{He1}}^{-1} &= -\exp(-\tau_{\text{He1}}) K_{\text{He1}}^{-1}, & K_{\text{He1}}^{-1} &= \frac{A_{2p_1}}{3(1 + 0.36 \gamma_{2p_1}^{0.86}) n_{\text{He}} (1 - X_{\text{He}}^+)}, & \tau_{\text{He1}} &= \frac{3A_{2p_1} n_{\text{He}} (1 - X_{\text{He}}^+)}{K_{\text{He1}}^{-1}}, \\
\gamma_{2p_1} &= \frac{3A_{2p_1} f_{\text{He}} c^2 (1 - X_{\text{He}}^+)}{8\pi \sigma_{\text{He1}} \sqrt{\frac{2\pi}{\beta m_{\text{He}} c^2}} (f_{\text{He1}}^{2p,1s})^3 (1 - X_{\text{H}}^+)}, & C_{\text{He1}} &= \frac{\exp(-\beta E_{\text{He1}}^{2p,2s}) + K_{\text{He1}} \Lambda_{\text{He1}} n_{\text{He}} (1 - X_{\text{He}}^+)}{\exp(-\beta E_{\text{He1}}^{2p,2s}) + K_{\text{He1}} (\Lambda_{\text{He1}} + \beta_{\text{He1}}) n_{\text{He}} (1 - X_{\text{He}}^+)}.
\end{aligned}$$

Second, Helium also includes contributions from triplet states (He_3):

$$\begin{aligned}
\alpha_{\text{He3}} &= \frac{q_3}{\sqrt{\frac{T_b}{T_2}} \left(1 + \sqrt{\frac{T_b}{T_2}} \right)^{1-p_3} \left(1 + \sqrt{\frac{T_b}{T_1}} \right)^{1+p_3}}, & \beta_{\text{He3}} &= \frac{4}{3} \frac{\alpha_{\text{He3}}}{\lambda_{\text{e}}^3} \exp(-\beta E_{\text{He3}}^{\infty,2s}), & \tau_{\text{He3}} &= \frac{3A_{2p_3} n_{\text{He}} (1 - X_{\text{He}}^+) (\lambda_{\text{He3}}^{2p,1s})^3}{8\pi H}, \\
\gamma_{2p_3} &= \frac{3A_{2p_3} f_{\text{He}} c^2 (1 - X_{\text{He}}^+)}{8\pi \sigma_{\text{He3}} \sqrt{\frac{2\pi}{\beta m_{\text{He}} c^2}} (f_{\text{He3}}^{2p,1s})^3 (1 - X_{\text{H}}^+)}, & C_{\text{He3}} &= \frac{A_{2p_3} \left(\frac{1 - \exp(-\tau_{\text{He3}})}{\tau_{\text{He3}}} + \frac{1}{3(1 + 0.66 \gamma_{2p_3}^{0.9})} \right) \exp(-\beta E_{\text{He3}}^{2p,2s})}{A_{2p_3} \left(\frac{1 - \exp(-\tau_{\text{He3}})}{\tau_{\text{He3}}} + \frac{1}{3(1 + 0.66 \gamma_{2p_3}^{0.9})} \right) \exp(-\beta E_{\text{He3}}^{2p,2s}) + \beta_{\text{He3}}}.
\end{aligned}$$

Every variable that does not occur on the left side of an equation is either a constant or a parameter. This includes Y_{He} , fudge factors and wavenumbers, frequencies and energies for atomic transitions. Some important variables are the baryon temperature T_b , photon

¹⁷ <https://www.astro.ubc.ca/people/scott/recfast.html>

temperature T_γ , mean molecular weight μ , baryon sound speed c_s^2 , optical depth κ , visibility function v and the free electron fraction X_e (conventionally relative to Hydrogen, so $X_e > 1$ in presence of Helium). Please consult the code and RECFAST references cited above for more details.

Unlike other RECFAST implementations, SymBoltz does not approximate the stiff Peebles equations at early times by Saha approximations (although X_{He}^{++} is given by a Saha equation at all times). This is not necessary with a good implicit ODE solver. SymBoltz sets $C_H = C_{\text{He}_1} = 1$ when $X_e \gtrsim 0.99$ to avoid numerical instability at early times. Atomic calculations are done in SI units and converted to SymBoltz' dimensionless units by factors of H_0 in SI units. The differential equation for T'_b is very stiff and sensitive to $T_b - T_\gamma$, but $T_b \approx T_\gamma$ in the early universe, so we rewrite it to a more stable differential equation for $\Delta T' = T'_b - T'_\gamma$ instead, initialize $\Delta T = 0$ and observe $T_b = \Delta T + T_\gamma$. The optical depth $\kappa(\tau) = \int_{\tau_0}^{\tau} \kappa'(\tau') d\tau'$ is really a line-of-sight integral into the past, but is integrated together with the background ODEs by initializing $\kappa(\tau_i) = 0$ to an arbitrary value, integrating the differential equation for κ' and subtracting the final value of $\kappa(\tau_0)$ (i.e. $\int_{\tau_0}^{\tau} = \int_{\tau_0}^{\tau_i} + \int_{\tau_i}^{\tau} = \int_{\tau_i}^{\tau} - \int_{\tau_i}^{\tau_0}$). There is no tight-coupling approximation.

Initial conditions are full ionization $X_H^+ = X_{\text{He}}^+ = 1$, thermal equilibrium $T_b = T_\gamma$ ($\Delta T = 0$), the arbitrary $\kappa = 0$, and adiabatic perturbations $\delta/(1+w) = -3\Psi/2$ and $\theta = k^2\tau\Psi/2$. The baryon species is parametrized by the reduced density $\Omega_0 = \frac{8\pi}{3}\rho_0$ today and the primordial Helium mass fraction Y_{He} .

SymBoltz solves thermodynamics equations together with the background equations, while some other codes treat these as separate stages. There is no meaningful performance improvement from doing this, as the size of the background (and thermodynamics) ODEs is so small. This makes a clear distinction between the background with all 0th order equations of motion, and the perturbations with all 1st order equations. It also makes it easy to create exotic models where the thermodynamics couple to the background, for example.

Note that RECFAST uses fitting functions to emulate the results of more physically accurate and expensive simulations. These are tuned to work for the Λ CDM model. SymBoltz would therefore benefit from including more physically accurate recombination models for safer use with modified models.

A.5. Photons (γ)

Photons are massless and therefore ultra-relativistic. Unlike non-relativistic particles, one must account for the direction $\cos\theta = \mathbf{p} \cdot \mathbf{k} / |\mathbf{p}||\mathbf{k}|$ of their momenta \mathbf{p} relative to the Fourier wavenumber \mathbf{k} . This results in a theoretically infinite hierarchy of equations for Legendre multipoles l , which in practice must be truncated at some maximum multipole l_{\max} :

$$\begin{aligned} T &= \frac{T_0}{a}, & w &= \frac{1}{3}, & c_s^2 &= w, & P &= \frac{\rho}{3}, & \rho &= \frac{\rho_0}{a^4}, & \delta &= F_0, & \theta &= \frac{3}{4}kF_1, & u &= \frac{\theta}{k}, & \sigma &= \frac{F_2}{2}, \\ F'_0 &= -kF_1 + 4\Phi', & F'_1 &= \frac{k}{3}(F_0 - 2F_2 + 4\Psi) + \frac{4}{3}\frac{\kappa'}{k}(\theta_\gamma - \theta_b), \\ F'_l &= \frac{k}{2l+1}(lF_{l-1} - (l+1)F_{l+1}) + F_l\kappa' - \delta_{l,2}\frac{\kappa'}{10}\Pi, & F'_{l_{\max}} &= kF_{l_{\max}-1} - \frac{l_{\max}+1}{\tau}F_{l_{\max}} + \kappa'F_{l_{\max}}, \\ G'_0 &= -kG_1 + \kappa'G_0 - \frac{\kappa'}{2}\Pi, & G'_l &= \frac{k}{2l+1}(lG_{l-1} - (l+1)G_{l+1}) + \kappa'G_l - \delta_{l,2}\frac{\kappa'}{10}\Pi, \\ G'_{l_{\max}} &= kG_{l_{\max}-1} - \frac{l_{\max}+1}{\tau}G_{l_{\max}} + \kappa'G_{l_{\max}}, & \Pi &= F_2 + G_0 + G_2, & \Theta_l &= \frac{F_l}{4}. \end{aligned}$$

The equations for F'_l and G'_l apply for $2 \leq l < l_{\max}$. There are no tight-coupling, radiation-streaming or ultra-relativistic fluid approximations. Initial conditions are adiabatic with $F_0 = -2\Psi$ (i.e. $\delta/(1+w) = -\frac{3}{2}\Psi$), $F_1 = \frac{2}{3}k\tau\Psi$ (i.e. $\theta = \frac{1}{2}k^2\tau\Psi$), $F_2 = -\frac{8}{15}\frac{k}{\kappa'}F_1$, $G_0 = \frac{5}{16}F_2$, $G_1 = -\frac{1}{16}\frac{k}{\kappa'}F_2$, $G_2 = \frac{1}{16}F_2$, and $F_l = -\frac{l}{2l+1}\frac{k}{\kappa'}F_{l-1}$ and $G_l = -\frac{l}{2l+1}\frac{k}{\kappa'}G_{l-1}$ for $3 \leq l \leq l_{\max}$. The species is parametrized by its temperature T_0 today, which in turn sets the density parameters $\Omega_0 = \frac{\pi^2}{15}\frac{(k_B T_0)^4}{(\hbar c)^3}\frac{8\pi G}{3H_0^2}$ and $\rho_0 = \frac{8\pi}{3}\Omega_0$ today.

A.6. Massless neutrinos (ν)

Massless neutrinos behave similarly to photons, but decouple from interactions with other species in the very early universe. One must only account for this interaction in initial conditions, while their evolution equations are a simpler case of the photons':

$$\begin{aligned} T &= \frac{T_0}{a}, & w &= \frac{1}{3}, & c_s^2 &= \frac{1}{3}, & P &= \frac{\rho}{3}, & \rho &= \frac{\rho_0}{a^4}, & \delta &= F_0, & \theta &= \frac{3}{4}kF_1, & \sigma &= \frac{F_2}{2}, \\ F'_0 &= -kF_1 + 4\Phi', & F'_1 &= \frac{k}{3}(F_0 - 2F_2 + 4\Psi), & F'_l &= \frac{k}{2l+1}(lF_{l-1} - (l+1)F_{l+1}), & F'_{l_{\max}} &= kF_{l_{\max}-1} - \frac{l_{\max}+1}{\tau}F_{l_{\max}}. \end{aligned}$$

The equations for F'_l apply for $2 \leq l < l_{\max}$. There is no ultra-relativistic fluid approximation. Initial conditions are adiabatic with $F_0 = -2\Psi$ (i.e. $\delta/(1+w) = -\frac{3}{2}\Psi$), $F_1 = \frac{2}{3}k\tau\Psi$ (i.e. $\theta = \frac{1}{2}k^2\tau\Psi$), $F_2 = \frac{2}{15}(k\tau)^2\Psi$ and $F_l = \frac{l}{2l+1}k\tau F_{l-1}$. The species is parametrized by the effective number N_{eff} , the reduced density $\Omega_0 = \frac{8\pi}{3}\rho_0$ and temperature T_0 today. If photons are present, they default to $T_{\nu 0} = \left(\frac{4}{11}\right)^{1/3}T_\gamma 0$ and $\Omega_{\nu 0} = N_{\text{eff}}\frac{7}{8}\left(\frac{4}{11}\right)^{4/3}\Omega_\gamma 0$.

A.7. Massive neutrinos (h)

Massive neutrinos are the most complicated species in the Λ CDM model (alongside baryon recombination). In essence, the species we have looked at so far have Boltzmann equations where the momenta of their distribution function can be integrated out analytically in non-relativistic and ultra-relativistic limits. This means that their stress-energy components are linked by trivial equations of state and sound speeds, for example, and their effect can be parametrized by a simple density parameter Ω_0 .

On the other hand, massive neutrinos have intermediate masses that fall between the non-relativistic and ultra-relativistic limits. Integrals over their distribution function must be computed numerically. This is very expensive if done naively, and it is extremely important to choose a quadrature scheme that minimizes the number of sampled points. Fortunately, the momentum integrals have a structure that can be exploited: they are all in the form weighted form $I[g(x)] = \int_0^\infty dx x^2 f(x) g(x)$, where $f(x) = 1/(e^x + 1)$ is the equilibrium distribution function and $g(x)$ is an arbitrary function of the dimensionless momentum $x = pc/k_B T$ (see [Ma & Bertschinger \(1995\)](#) for more details). One can generally approximate $I[g(x)] \approx \sum_i W_i g(x_i)$ with a weighted quadrature scheme with points x_i and weights W_i (more on this after the equations). In other words, the integral operator $\int_0^\infty dx x^2 f(x)$ is effectively replaced by the discrete summation operator $\sum_i W_i$ for some weights W_i .

On top of this, perturbations are also expanded in Legendre multipoles l up to a cutoff l_{\max} :

$$\begin{aligned}
T &= \frac{T_0}{a}, & x &= \frac{pc}{k_B T}, & y &= \frac{mc^2}{k_B T}, & E_i &= \sqrt{x_i^2 + y^2}, & f &= \frac{1}{1 + e^x}, & \frac{d \ln f}{d \ln x} &= -\frac{x}{1 + e^{-x}}, \\
I_\rho &= \sum_i W_i E_i, & I_P &= \sum_i W_i \frac{x_i^2}{E_i}, & \rho &= \frac{N}{\pi^2} \frac{(k_B T)^4}{(\hbar c)^3} \frac{G}{(H_0 c)^2} I_\rho, & P &= \frac{N}{3\pi^2} \frac{(k_B T)^4}{(\hbar c)^3} \frac{G}{(H_0 c)^2} I_P, & w &= \frac{P}{\rho}, \\
\psi'_{i,0} &= -k \frac{x_i}{E_i} \psi_{i,1} - \Phi' \left(\frac{d \ln f}{d \ln x} \right)_i, & \psi'_{i,1} &= \frac{k}{3} \frac{x_i}{E_i} (\psi_{i,0} - 2\psi_{i,2}) - \frac{k}{3} \frac{E_i}{x_i} \Psi \left(\frac{d \ln f}{d \ln x} \right)_i, \\
\psi'_{i,l} &= \frac{k}{2l+1} \frac{x_i}{E_i} (l\psi_{i,l-1} - (l+1)\psi_{i,l+1}), & \psi_{i,l_{\max}+1} &= \frac{2l_{\max}+1}{k\tau} \frac{E_i}{x_i} \psi_{i,l_{\max}} - \psi_{i,l_{\max}-1}, \\
I_0 &= \sum_i W_i E_i \psi_{i,0}, & I_1 &= \sum_i W_i x_i \psi_{i,1}, & I_2 &= \sum_i W_i \frac{x_i^2}{E_i} \psi_{i,2}, & \delta &= \frac{I_0}{I_\rho}, & \sigma &= \frac{2I_2}{3I_\rho + I_P}, & u &= \frac{3I_1}{3I_\rho + I_P}, & \theta &= ku.
\end{aligned}$$

Initial conditions are $\psi_{i,0} = -\frac{1}{4}(-2\Psi) \left(\frac{d \ln f}{d \ln x} \right)_i$, $\psi_{i,1} = -\frac{1}{3} \frac{E_i}{x_i} \frac{1}{2} k \tau \Psi \left(\frac{d \ln f}{d \ln x} \right)_i$, $\psi_{i,2} = -\frac{1}{2} \frac{1}{15} (k \tau)^2 \Psi \left(\frac{d \ln f}{d \ln x} \right)_i$ and $\psi_{i,l} = 0$. This integrates to adiabatic $\delta/(1+w)$, θ and σ similarly to massless neutrinos. Free parameters are the temperature today T_0 , mass m of a single neutrino and degeneracy factor $N = \sum_{i=1}^N m_i/m$ for describing multiple neutrinos with equal mass. The degeneracy factor defaults to $N = 3$, and the temperature to $T_{h0} = (\frac{4}{11})^{1/3} T_{\gamma 0}$ if photons are present, as for massless neutrinos.

Here the equation for $\psi'_{i,l}$ applies for $2 \leq l \leq l_{\max}$, and expressions $g_i = g(x_i)$ indexed by i are evaluated with the momentum quadrature point $x = x_i$. The reduction to dimensionless momenta $x = pc/k_B T$ (the argument of \exp in f) is deliberate because it makes numerics more well-defined and the quadrature scheme independent of m and all other cosmological parameters.

SymBoltz automatically computes momentum bins x_i and quadrature weights W_i with N -point Gaussian quadrature. First, by default, the following substitution is applied to the momentum integral:

$$\int_0^\infty dx x^2 f(x) g(x) = \int_{u(0)}^{u(\infty)} du x'(u) x(u)^2 f(x(u)) g(x(u)) \quad \text{with} \quad u(x) = \frac{1}{1 + \frac{x}{L}}.$$

This substitution achieves two things: the scaling x/L brings the dominant integral contributions well within $x/L \ll 1$ if L is chosen to be a characteristic decay ‘length’ of the distribution function, and the rational part $1/(1+x/L)$ maps the infinite domain $x \in (0, \infty)$ to the finite domain $u \in (0, 1)$, which can be integrated numerically. The substituted integrand is then passed to an adaptive algorithm in [QuadGK.jl¹⁸](#) that computes quadrature points u_i and weights W_i by performing weighted integrals against several test functions $g(x)$. Finally, the corresponding momenta $x_i = x(u_i)$ are returned along with the weights W_i , from which one can approximate the integral $I[g(x)] \approx \sum_i W_i g(x_i)$ against any $g(x)$.

SymBoltz tests this numerical quadrature scheme against the analytical result $I[x^{n-2}] = \int_0^\infty dx x^n / (e^x + 1) = (1 - 2^{-n}) \zeta(n+1) \Gamma(n+1)$ for $2 \leq n \leq 8$. We assume this to be a reasonable test for the integrals encountered in the equations above. Agreement is excellent with $L = 100$, which yields relative errors below 10^{-6+n-N} for all $2 \leq n \leq 8$ and $1 \leq N \leq 5$. SymBoltz defaults to $N = 4$ momenta, for which this relative error is less than 10^{-6} for $n \leq 4$, for example. It also agrees well with CLASS using default settings.

Note that this momentum quadrature strategy is generic with respect to the distribution function $f(x)$ and substitution $u(x)$, so it can easily be modified for other particle species whose distribution function cannot be integrated out.

CAMB ([Lewis 2025](#)) and CLASS ([Lesgourgues & Tram 2011](#)) apply similar weighted quadrature strategies. They also get away with only a handful of sampled momenta, but the precise details of the computation differ slightly. For reference, here are points and weights computed by SymBoltz for $1 \leq N \leq 8$ momenta:

¹⁸ <https://github.com/JuliaMath/QuadGK.jl>

| N | x_1 | x_2 | x_3 | x_4 | x_5 | x_6 | x_7 | x_8 |
|-----|---------|---------|---------|----------|----------|----------|----------|----------|
| 1 | 3.12273 | | | | | | | |
| 2 | 2.07807 | 5.94834 | | | | | | |
| 3 | 1.56110 | 4.22902 | 8.86258 | | | | | |
| 4 | 1.24461 | 3.30909 | 6.57536 | 11.80351 | | | | |
| 5 | 1.02955 | 2.71805 | 5.27853 | 9.03363 | 14.74043 | | | |
| 6 | 0.87373 | 2.30142 | 4.41479 | 7.39595 | 11.55088 | 17.65818 | | |
| 7 | 0.75572 | 1.99028 | 3.79064 | 6.27323 | 9.60568 | 14.09716 | 20.54878 | |
| 8 | 0.66337 | 1.74848 | 3.31580 | 5.44442 | 8.24194 | 11.87257 | 16.65452 | 23.40806 |
| N | W_1 | W_2 | W_3 | W_4 | W_5 | W_6 | W_7 | W_8 |
| 1 | 1.80309 | | | | | | | |
| 2 | 1.30306 | 0.50002 | | | | | | |
| 3 | 0.84813 | 0.88596 | 0.06899 | | | | | |
| 4 | 0.55272 | 0.99943 | 0.24384 | 0.00709 | | | | |
| 5 | 0.36868 | 0.95311 | 0.43658 | 0.04409 | 0.00063 | | | |
| 6 | 0.25275 | 0.84165 | 0.58496 | 0.11736 | 0.00632 | 0.00005 | | |
| 7 | 0.17792 | 0.71541 | 0.67227 | 0.21284 | 0.02386 | 0.00079 | 0.00000 | |
| 8 | 0.12832 | 0.59663 | 0.70569 | 0.31144 | 0.05685 | 0.00406 | 0.00009 | 0.00000 |

A.8. Cosmological constant (Λ)

The cosmological constant is equivalent to a very simple species without perturbations:

$$w = -1, \quad \rho = \rho_0, \quad P = -\rho, \quad \delta = 0, \quad \theta = 0, \quad \sigma = 0, \quad u = 0.$$

It is parametrized by the reduced density $\Omega_0 = \frac{8\pi}{3}\rho_0$ today. This is set to $\Omega_{\Lambda 0} = 1 - \sum_{s \neq \Lambda} \Omega_{s0}$ if all species s have a Ω_{s0} parameter and General Relativity is the theory of gravity. This constraint comes from the 1st Friedmann equation today.

A.9. Primordial power spectrum (I)

SymBoltz computes the inflationary primordial power spectrum parametrized by the amplitude A_s and tilt n_s :

$$P_0(k) = \frac{2\pi^2}{k^3} A_s \left(\frac{k}{k_p} \right)^{n_s - 1}.$$

A.10. Matter power spectrum

SymBoltz computes the matter power spectrum for some desired set of species s , which are presumably matter-like at late times (e.g. $s \in \{c, b, h\}$):

$$P(k, \tau) = P_0(k) |\Delta(\tau, k)|^2 \quad \text{with} \quad \Delta = \delta + \frac{3\mathcal{H}}{k^2} \theta = \frac{\sum_s \delta \rho_s}{\sum_s \rho_s} + \frac{3\mathcal{H}}{k^2} \frac{\sum_s (\rho_s + P_s) \theta_s}{\sum_s (\rho_s + P_s)}.$$

Here Δ is the total gauge-independent overdensity with total δ and θ computed by summing the components of the energy-momentum tensor that are additive.

A.11. CMB power spectrum and line-of-sight integration

SymBoltz finds photon temperature and polarization multipoles today for any l by computing the line-of-sight integrals

$$\Theta_l^T(\tau_0, k) = \int_{\tau_i}^{\tau_0} S_T(\tau, k) j_l(k(\tau_0 - \tau)) d\tau \quad \text{with} \quad S_T = v \left(\frac{\delta_\gamma}{4} + \Psi + \frac{\Pi_\gamma}{16} \right) + e^{-\kappa} (\Psi + \Phi)' + \frac{(vu_b)'}{k} + \frac{3}{16k^2} (v\Pi_\gamma)'',$$

$$\Theta_l^E(\tau_0, k) = \sqrt{\frac{(l+2)!}{(l-2)!}} \int_{\tau_i}^{\tau_0} S_E(\tau, k) \frac{j_l(k(\tau_0 - \tau))}{(k(\tau_0 - \tau))^2} d\tau \quad \text{with} \quad S_E = \frac{3}{16} v\Pi_\gamma.$$

As first suggested by [Seljak & Zaldarriaga \(1996\)](#), this approach enables cheap computation for any l after integrating the perturbation ODEs with only a few $l \leq l_{\max}$. This drastically speeds up the computation over including all l in an enormous set of coupled perturbation ODEs. SymBoltz performs the integrals with the trapezoid method using the substitution $u(\tau) = \tanh(\tau)$, which adds more points in the early universe when sampled uniformly, using 768 points by default. Here j_l are the spherical Bessel functions

of the first kind. SymBoltz is not yet generalized to non-flat geometries, where they are replaced by hyperspherical functions. The cross-correlated angular spectrum between $A, B \in \{T, E\}$ is then computed from

$$C_l^{AB} = \frac{2\pi}{l(l+1)} D_l^{AB} = \frac{2}{\pi} \int_0^\infty dk k^2 P_0(k) \Theta_l^A(\tau_0, k) \Theta_l^B(\tau_0, k).$$

This integral is also performed with the trapezoid method. The point $(k, \Theta) = (0, 0)$ is included manually, for which the numerical solution to the perturbation ODEs is ill-defined. By default, the Θ_l are sampled on a fine grid of wavenumbers with spacing $\Delta k = 2\pi/2\tau_0$, which interpolates from solved perturbation modes on a coarse grid $\Delta k = 8/\tau_0$. Both grids range between $0.1l_{\min}/\tau_0 \leq k \leq 3l_{\max}/\tau_0$, where l_{\min} and l_{\max} are the angular spectrum's minimum and maximum requested multipoles.

A.12. Adaptive source function refinement

SymBoltz can optionally refine source functions $S(\tau, k)$ in k , such as when computing the matter or CMB power spectra.

First, the source function $S_i(\tau) = S(\tau, k_i)$ is found on an initial grid of wavenumbers k_i by integrating their perturbations. The method then iterates over each interval (k_i, k_{i+1}) , integrates the perturbations for the center $k_{i+1/2} = (k_i + k_{i+1})/2$ and finds $S_{i+1/2}(\tau) = S(\tau, k_{i+1/2})$. The idea is then to compare this to a linearly interpolated source $S_{\text{int}}(\tau) = (S_i(\tau) + S_{i+1}(\tau))/2$ with some error measure err , for example from $\text{err}^2 = \int d\tau (S_{\text{int}}(\tau) - S_{i+1/2}(\tau))^2$. If the interpolation is poor and err is greater than some absolute and relative tolerances, the left and right half-intervals $(k_i, k_{i+1/2})$ and $(k_{i+1/2}, k_{i+1})$ are recursively refined in the same way.

This gives $S(\tau, k)$ by integrating as few k -modes as possible. Instead of manually creating a non-uniform k -grid with many hyperparameters, the process is controlled by only one tolerance. It parallelizes over each interval and can also be done in $\log k$.

Appendix B: Precision parameters for CLASS

When comparing results to CLASS in section 3, we use CLASS version 3.3.4 with the following precision parameters:

```
tight_coupling_approximation = 5 # compromise_CLASS; cannot disable TCA
tight_coupling_trigger_tau_c_over_tau_h = 0.01 # turn off TCA earlier
tight_coupling_trigger_tau_c_over_tau_k = 0.001 # turn off TCA earlier
radiation_streaming_approximation = 3 # turn off RSA
ncdm_fluid_approximation = 3 # turn off NCDMFA
ur_fluid_approximation = 3 # turn off UFA

evolver = 1 # for implicit ndf15; 0 for explicit rk
tol_perturbations_integration = 1.0e-6 # less noise; varied in work-precision diagram
tol_ncdm_newtonian = 1.0e-5 # default sampling of massive neutrino momenta
background_Nloga = 6000 # for stable derivatives
```

We run CLASS with `output = mPk` to compute only $P(k)$, and `output = tCl, pCl` to compute only C_l^{TT} , C_l^{EE} and C_l^{TE} with the code's most specialized and optimized paths. CLASS and SymBoltz are configured to use the same Newtonian gauge, l_{\max} for all species, RECFAST recombination model, tanh-like reionization parametrization, $w_0 w_a$ dark energy equations and cosmological parameter values. The settings above disable as many approximations as possible and reduce the impact of the tight-coupling approximation, which cannot be disabled. We had to decrease the parameter `background_Nloga` from the default value 40000 to make the derivatives in fig. 4 stable. This parameter controls the number of points used for splining background functions in the perturbations. Its default value was changed from 3000 to 40000 in 2023, but we suspect that the increased density in points makes the splines oscillate from numerical noise. Likewise, the tolerance for the perturbations ODEs is set one notch smaller than the default 10^{-5} to make the output stable. We use CLASS' default sampling of massive neutrino momenta, as discussed in section 4.

When running CLASS with all approximations on in table 1 and fig. 7, the first block of parameters above are not used. In the work-precision comparison in fig. 7, we also vary `tol_perturbations_integration` and `evolver` as described in the figure.

Appendix C: Testing and comparison to CLASS

SymBoltz' code repository is set up with continuous integration that runs several tests and builds updated documentation pages every time changes to the code are committed. In particular, this compares the solution for Λ CDM with CLASS for many variables solved by the background, thermodynamics and perturbations (using the options `write_background`, `write_thermodynamics` and `k_output_values`). These are the basis for all derived quantities like luminosity distances, matter and CMB power spectra, which are also compared. The checks pass when the quantities agree within a small tolerance. We do not compare directly against more codes like CAMB, but CLASS has already been compared extensively with CAMB with excellent agreement (Lesgourges 2011b). The comparison takes a lot of space and is not included here, but is found in the documentation linked from SymBoltz' repository.

Another test checks that integration of the background and perturbations equations are stable throughout parameter space. As the equations are very stiff and SymBoltz does not rely on approximations for relieving it, one could imagine that the integration would be stable for some parameter values and unstable for others. The test creates a box in parameter space $\pm 50\%$ around a fiducial set of realistic parameter values, draws several sets of parameter values from that space with Latin hypercube sampling (to efficiently cover parameter space) and integrates the background and perturbations for each such set. All parameter samples are found to integrate successfully without warnings and errors.